Drought impacts on the electricity system, emissions, and air quality in the western US

Minghao Qiu[1,2,*], Nathan Ratledge[3], Inés Azevedo[4], Noah S. Diffenbaugh[5], Marshall Burke[5,6,7]

1 Department of Earth System Science, Stanford University, Stanford, CA, USA

2 Center for Innovation in Global Health, Stanford University, Stanford, CA, USA

3 Emmett Interdisciplinary Program in Environment and Resources, Stanford University, Stanford, CA, USA

4 Department of Energy Science and Engineering, Stanford University, Stanford, CA, USA

5 Doerr School of Sustainability, Stanford University, Stanford, CA, USA

6 Center on Food Security and the Environment, Stanford University, Stanford, CA, USA

7 National Bureau of Economic Research, Cambridge, MA, USA

***** To whom correspondence should be addressed. E-mail: mhqiu@stanford.edu

Abstract

The western United States has experienced severe drought in recent decades, and climate models project increased drought risk in the future. This increased drying could have important implications for the region's interconnected, hydropower-dependent electricity systems. Using power-plant level generation and emissions data from 2001-2021, we quantify the impacts of drought on the operation of fossil fuel plants and the associated impacts on greenhouse gas emissions, air quality, and human health. We find that under extreme drought, electricity generation from individual fossil fuel plants can increase up to 65% relative to average conditions, mainly due to the need to substitute for reduced hydropower. Over 54% of this drought-induced generation is trans-boundary, with drought in one electricity region leading to net-imports of electricity and thus increased pollutant emissions from power plants in other regions. These drought-induced emissions increases have detectable impacts on local air quality, as measured by proximate pollution monitors. We estimate that the monetized costs of excess mortality and greenhouse gas emissions from drought-induced fossil generation are 1.2-2.5x the reported direct economic costs from lost hydro production and increased demand. Combining climate model estimates of future drying with stylized energy-transition scenarios suggests that these drought-induced impacts are likely to remain large even under aggressive renewables expansion, suggesting that more ambitious and targeted measures are needed to mitigate the emissions and health burden from electricity sector during droughts.

Climate change can influence energy systems by altering energy supply, demand, and transmission, leading to significant economic and environmental impacts (1–5). For instance, existing work highlights how a changing climate will affect electricity demand and energy expenditure (6, 7), how it can influence how much of a given energy source (e.g. hydropower) can be utilized (8–10), and how it can influence the operations of thermal power plants (11). Many of these insights are then incorporated into energy system models to estimate the overall impacts of climate change on the energy supply, demand, and system cost (12).

Yet the overall societal costs of climate-related disruptions to the energy system could extend beyond the channels explored in existing work. In particular, climate disruptions could result in increases in electricity generation from fossil fuel sources, if a changing climate induces large changes in energy demand and/or supply, as existing work suggests, and if marginal electricity generation source used to cover short-run increases in demand or decreases in supply remains reliant on fossil fuels. Increased fossil generation could then result in increased greenhouse gas (GHG) and air pollutant emissions, with emissions increases perhaps occurring far from the location of the climate shock, given the spatially interconnected nature of many energy systems. The associated economic and health impacts of these climate-induced emissions are unaccounted for in existing analyses.

In this paper, we study the impacts of drought on the electricity system and the consequent effects on GHG emissions, air quality, and human health in the western United States (US). Drought could influence the electricity generation and emissions of fossil fuel power plants through a variety of compounding pathways. Drought reduces runoff and electricity generation from hydropower (12, 13), while accompanying heatwaves can influence electricity demand (14, 15). Accompanied weather patterns during droughts can also influence electricity supply from non-hydro renewable energy sources, e.g., drought-induced wildfire smoke could reduce solar generation (16), which can then influence generation and emissions from fossil fuel plants. As many fossil fuel plants require extensive amounts of cooling water, a scarcity of cooling water can also decrease the operating efficiency and electricity supply from those impacted plants (11, 14, 17). More importantly, when multiple regions are connected through the electricity transmission networks, drought conditions in one region could lead to changes in generation from fossil fuel plants in another region (18, 19). These multiple pathways between drought and operation of fossil fuel plants make it difficult to understand the emission and air quality impacts of drought on the electricity system *ex ante*.

To study the impacts of drought on the electricity system, we focus on the 11 US states which are connected to the Western Interconnection. The western US has experienced record-breaking drought

conditions since 2000 and a declining trend in total runoff (figure 1A), influenced by anthropogenic climate change (20, 21). Reduced runoff has substantial implications for the electricity system in the western US, given that hydro accounts for 23% of the electricity generation in this region (22) and that there is a very close coupling between runoff anomalies and hydro generation (figure 1B). The western US faces significant challenges under a changing climate as climate models project significant increases in drought risks due to increased co-occurrence of high temperature and low precipitation conditions (20, 23). Despite having lower air pollutant and GHG emissions per unit of electricity generation compared to the rest of US, 60% of the regional electricity supply still comes from over 800 fossil fuel power plants, including 108 coal or oil-based power plants with high CO_2, SO_2 and NO_x emissions (figure 1C).

Recent droughts in this region have attracted wide attention (18, 24–28), but much less is understood about the potential impacts on emissions, air quality, and human health. Using energy system models or state-level data analysis, a few studies have found significant increases in CO_2 emissions from the power sector during droughts (25, 26, 29, 30). Very few studies have quantified the impacts of drought on air pollutant emissions from fossil fuel plants, and these estimates are often aggregated at the regional or state level (30, 31). Accurate accounting for the emissions and health impacts of drought-induced fossil fuel generation is challenging, as it needs to account for both the heterogeneous responses across different power plants at different locations, as well as trans-boundary impacts through the inter-regional exchange of electricity. Future policy and investment would also benefit from projections of the emissions impacts under future climate change and potential transitions in the electricity sector (e.g., expansion of renewable energy); however, there exists no studies conducting such projections using empirically-grounded relationships.

Here, we estimate the impacts of drought on electricity generation and emissions from fossil fuel plants in the western US and the associated air quality and health effects, using empirical data on plant-level generation and emissions, runoff, and observational air quality measured by surface monitors from 2001-2021. Our analysis directly accounts for the trans-boundary impacts of drought on fossil fuel generation and pollutant emissions, due to the import/export of electricity across three electricity regions (figure 1C, following definitions of the Energy Information Agency). We first develop a statistical model between plant-level electricity generation and runoff anomalies in each of the three electricity regions. For each plant, we calculate the drought-induced electricity generation, defined as the changes in electricity generation as a result of the runoff anomalies (relative to the 1980-2021 average). As drought impacts on individual fossil fuel plants vary as a result of

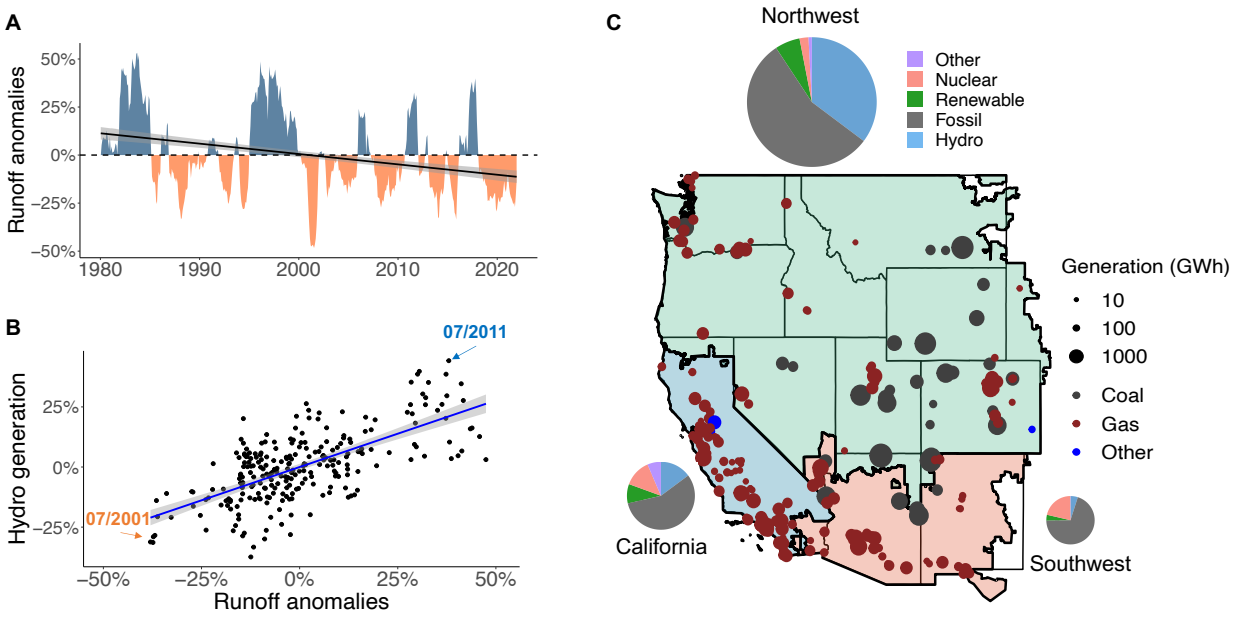

Figure 1: **Drought conditions and the electricity system in the western US.** Panel A: the declining trend of regional runoff anomalies of western US from 1980 to 2021. Panel B: relationship between monthly hydro generation anomalies (deviations relative to the monthly mean) and monthly runoff anomalies in the western US. Panel C: fossil fuel power plants in the western US in our sample during the studied period (2001-2021). Western US is divided into three electricity regions: California (CA), Northwest (NW), and Southwest (SW). Pie charts in panel C show the percentage of electricity generation from different generating technologies, averaged over 2001 to 2021 (size of the pie is proportional to the total electricity generation in each region).

their operational status, locations, and fuel type, we estimate drought impacts at a disaggregated level – specifically on each set of power plants that are located in the same electricity balancing area and use the same fuel type.

To estimate the impacts on air quality and related health damages, we quantify the changes in measured surface $PM_{2.5}$ that are attributable to drought-induced changes in SO_2 and NO_x emissions from fossil fuel plants. We specifically focus on surface $PM_{2.5}$ that is not related to wildfire smoke, as wildfire is more prevalent during drought periods and it contributes substantially to surface $PM_{2.5}$ (see Methods). We quantify whether predicted drought-induced emissions affect surface $PM_{2.5}$ concentration measured at nearby air pollution monitors. We then calculate the monetized damages from excess mortality due to observed $PM_{2.5}$ changes using an empirically derived concentration response function (CRF) that relates short-term changes in air pollution to mortality (*32*) and a value of statistical life of $10.95 million (year 2019 dollars) recommended by the US EPA (*33*).

We further quantify the monetized damages of drought-induced GHG emissions by accounting for increased CO_2 emissions using the social cost of carbon ($117 per ton, year 2020 dollars) (34), and methane (CH_4) leakages using a 2.3% leakage rate across the life cycle of the gas production and usage (35) and the social cost of methane ($1257 per ton, year 2020 dollars) (34).

Finally, to assess potential impacts under future climate and energy production scenarios, we combine our empirical estimates of plant-level emission changes with climate projections and stylized electricity sector scenarios. We use the average 2030-2059 projected runoffs (surface + sub-surface) from The Coupled Model Intercomparison Project Phase 6 (CMIP6) climate model ensemble. We consider three potential scenarios in the electricity sectors using results from existing energy system model projections (36, 37): replacing coal power plants with natural gas plants, increased penetration of carbon capture and storage (CCS), and increased penetration of renewable energy and battery technology. For the renewable energy scenario, we use the "Low Renewable Cost" scenario from National Renewable Energy Lab's projections of the U.S. electric sector through 2050 (36), which projects the average and marginal energy source in the electricity sector under the lower end of the projected renewable energy cost. As a baseline for these comparisons, we quantify the damages under a high climate forcing scenario (SSP3-7.0) with no changes in the electricity sector (the "reference scenario"). We then quantify the differences in damages under alternative climate scenarios as well as lower-carbon electricity sector scenarios.

Results

Drought increases electricity generation from fossil fuel plants

Compared to the average conditions in 1980-2021, the electricity generation from the fossil fuel plants on average increased by 35%, 11%, and 9.5%, in California (CA), Northwest (NW), and Southwest (SW) in the driest months during the study period (see figure 2). Importantly, we find the combined effect of droughts on fossil generation across the three regions ("total effect") is substantially larger than the effect of drought on the fossil generation in the same region alone ("local effect"). Increases in fossil generation due to drought conditions occurring in the neighboring electricity regions account for 56% of the total generation increases in CA during the drought periods, along with 30% of the total generation increases in NW, and 95% of the generation increase in SW. As shown in figures 2D to 2F, drought occurring in the NW could lead to increases in fossil fuel generation in all three electricity regions, while CA droughts lead to increases in fossil fuel generation from power

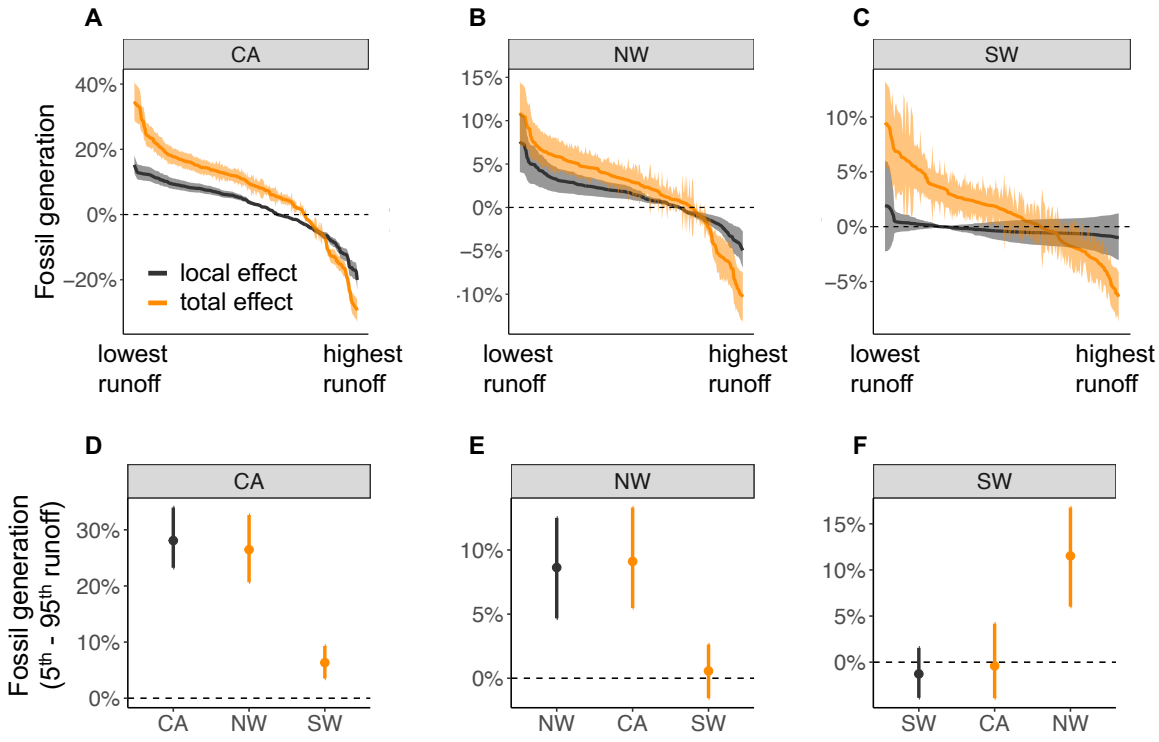

Figure 2: **Drought increases electricity generation from fossil fuel plants with substantial trans-boundary effects.** Panels A to C: relative changes in monthly fossil generation in each region due to runoff changes in our study period. X-axis is sorted by the changes in fossil fuel generation, from months with the highest drought-induced generation (lowest runoff) on the left to the months with the lowest generation (highest runoff) on the right. Black lines show the "local effect" which only accounts for the impact of runoff on power plants in the same region. Orange lines show the "total effect" which accounts for the impacts resulting from runoff changes in all three regions. Panels D to F: changes in fossil generation in one electricity region (each panel) due to the 5th to 95th percentile change of runoff anomalies in each of the three regions (x-axis of each panel). The shades in panels A-C and error bars in panels D-F show the 95% confidence intervals of the estimated generation changes.

plants in CA and NW. Our estimation results are consistent across alternative specifications of the econometric models, models using alternative drought indices, and the choices of data inclusion criterion (see figure S1, S2, S3).

The trans-boundary effects of drought on fossil fuel generation are largely driven by the changes in the import/export of electricity due to drought-induced supply or demand shocks. Neighboring regions that are connected to the drought regions increase fossil fuel generation from their own plants to make up for shortfall in the drought region. We corroborate these findings using a separate dataset

on the import and export of electricity between these three regions (*38*), and find that a significant drought (defined as a deficit in runoff between the 5th and 95th percentile of runoff anomalies) in the NW led to a 23% increase of net export of electricity from CA to NW, and a 7.2% increase of net export from the SW to NW (see figure S4). Magnitudes of the import/export changes are consistent with the trans-boundary effects of drought-fossil generation quantified above (a 26.5% increase in CA fossil generation due to NW droughts, and a 11.5% increase in SW fossil generation due to NW droughts). These results suggest that when hydropower production is reduced in the NW under drought, less power is available for export to either CA or SW and therefore fossil fuel plants in CA or SW would need to increase their electricity generation to fill this gap.

To further understand the mechanisms between runoff and fossil fuel generation, we use causal mediation analysis in CA and NW where the "local effects" of drought on fossil generation are significant and substantial (see figure S6). We find that the need to substitute for changes in hydro power is the leading mechanism that explains the runoff – fossil generation relationship. Surprisingly, we find that increases of fossil generation during low runoff periods are not empirically related to the changes in the electricity demand. In the discussion section, we briefly discuss the potential reasons and its implications. In CA, we further observe some evidence that a small fraction of the increases in fossil generation could be due to reductions in renewable generation, consistent with evidence of reduction in solar generation due to wildfire smoke (which often coincide with droughts) and the reduction in wind power due to low wind speed during drought episodes (*39*–*41*). We also find some evidence that the drought-induced emissions increases at the fossil fuel plants are possibly offset by increases in ambient temperature at the plant locations, suggesting potential generation curtailment due to high temperature conditions (see figure S6). To further test whether the hydro displacement is the dominant channel between runoff and fossil fuel generation, we perform a placebo test that applies the same model to Texas and Florida, two electricity regions that are largely isolated from the rest of the country and have little hydro electricity capacity. There, we find no effects of regional runoff changes on generation and emissions from fossil fuel plants (see table S1).

Drought-induced emissions increase surface $PM_{2.5}$ near fossil fuel plants

When accounting for the plant-level heterogeneity, we find that the drought-induced emissions account for ∼12% of the total regional CO_2 emissions from the electricity sector, ∼6% of the total NO_x emissions, and ∼8% of the SO_2 emissions during extreme drought periods (e.g., spring and summer during 2001). Relative changes in SO_2 and NO_x emissions are smaller than CO_2 emissions

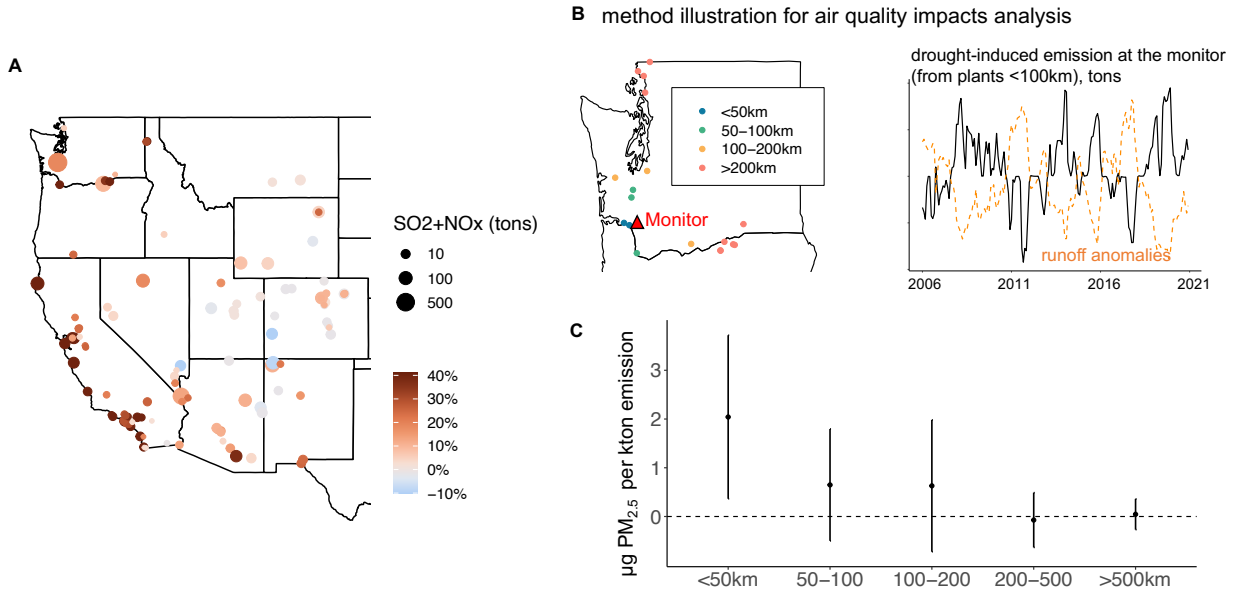

Figure 3: **Drought-induced emissions increase nearby surface $PM_{2.5}$ concentration.** Panel A: predicted drought-induced emissions (SO_2 + NO_x) from each fossil plant due to runoff anomalies in 2001, an extremely dry year. Colors show the percentage changes relative to the total plant emissions. Panel B: illustration of our method to quantify impacts of drought-induced emissions on $PM_{2.5}$ concentration measured at surface air quality monitors, using a specific monitor in Washington as example. For each monitor, we calculate total drought-induced emissions from all fossil fuel plants within a given distance of the monitor (e.g. 100km), and quantify the impacts on surface air quality due to changes in emissions within that distance. Panel C shows the impacts of drought-induced emission from power plants in each distance bin on surface $PM_{2.5}$ measured at the monitors (the bars show the 95% confidence interval).

due to the relatively smaller impacts of droughts on the large high-emitting coal power plants. However, some individual power plants experience larger changes in SO_2 and NO_x (figure 3A). For example, in an extremely dry year like 2001, we predict that roughly 20% of plants would increase their SO_2 and NO_x emissions by at least 30%, or more than triple the regional average. These results highlight the substantial local heterogeneity in emissions impacts from a common regional drought shock.

Drought-induced emissions of SO_2 and NO_x from fossil fuel plants increases the surface $PM_{2.5}$ near the power plants (in particular, within a 50km radius), while, as expected, the effects gradually decay as the distance between the monitor and power plant increases (figure 3C; also see figure 3B and Method for method illustrations). We also find evidence that suggests increases in surface $PM_{2.5}$ are more likely to be associated with drought-induced emissions from plants at the upwind location

of the monitor, further strengthening our causal claims (see figure S7). Our estimation results are largely robust to alternative specifications of the empirical models (see figure S8). We also calculate the impacts on surface $PM_{2.5}$ using the reduced-complexity air quality model, the Intervention Model for Air Pollution (InMAP), which is commonly used to evaluate impacts of emission changes on $PM_{2.5}$ (*42*). Using the same set of drought-induced emission, InMAP estimates a significant increase in surface $PM_{2.5}$, although with a substantially smaller magnitude than our empirically-derived estimates (see figure S11 and the discussion section).

Monetized economic and health impacts of historical droughts

We value the total health and economic damages of drought-induced fossil electricity generation by monetizing the impact of predicted changes in air pollution, CH_4 leakage, and CO_2 emissions when drought strikes, applying our estimates backward over the observed drought time series. As most of the recent 20 year period is drier than the 1980-2021 long-term average, we calculate that the western US has experienced a total net damage of $20 billion during this period. Drought-induced CO_2 emissions account for $14 billion, or 70% of the total damage. $PM_{2.5}$-associated mortality accounts for $5.1 billion (25% of the total damage), and CH_4 leakages accounts for $0.9 billion (5% of the total damage). Results calculated with alternative CRFs and SCC rate are shown in the SI.

Despite the consequential total damage from recent historical droughts, annual damages declined markedly after 2001. This is largely driven by the declining emission factor of fossil fuel electricity generation (i.e. emissions of NO_x, SO_2, and CO_2 per unit of electricity generation) over the last 20 years. NO_x and SO_2 emission factors in the western US have declined by 8-10 fold primarily due to the transition from coal to natural gas and the installation of scrubbers (*44*, *45*). The CO_2 emission factor also declined by 40% – a magnitude smaller than SO_2 or NO_x since natural gas plants are still significant carbon emitters and policies rarely target the stack-level emissions of CO_2 within the fossil fuel plants.

We find that installation of scrubbers at high-emitting plants near the population centers lead to marked reduction in the $PM_{2.5}$-related health damages. For example, one power plant (which includes two coal-fired units) in Washington state was responsible for 26% of the total drought-induced $PM_{2.5}$ damage in 2001 in the western US (see figure S12). However, drought-induced $PM_{2.5}$ damages associated with this plant decreased by 90% after the installation of scrubbers at the plant in 2002, contributing to a large part of the decline in total $PM_{2.5}$ damage. In the more recent years (e.g., 2018-2021), most of the monetized damages of the drought-induced fossil

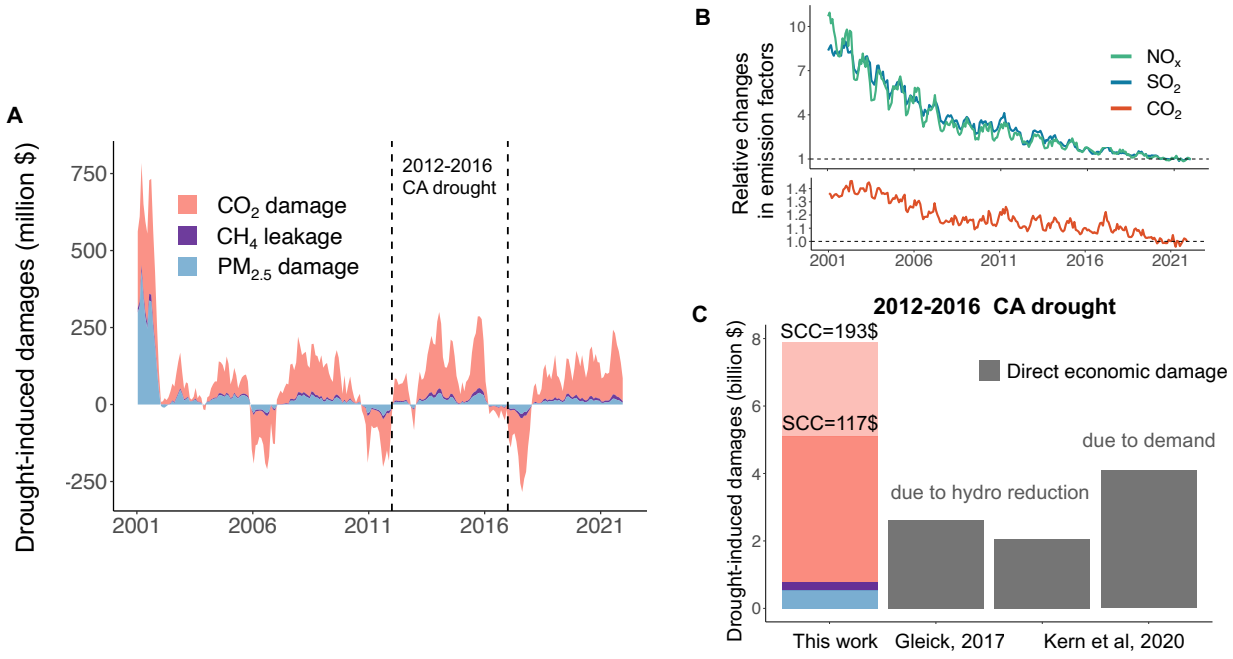

Figure 4: **Monetized economic and health impacts of drought-induced fossil fuel generation.** Panel A: monetized damages from extra CO_2 emissions, CH_4 leakage, and $PM_{2.5}$-related mortalities, due to runoff changes (relative to the 1980-2021 average). Monetized values are calculated using a social cost of carbon value of \$117 per ton, a social cost of methane value of \$1257 per ton (year 2020 dollars) from US EPA (*34*) and a value of statistical life of \$10.95 million per mortality (year 2019 dollars). Panel B: declines in annual monetized damages over time are a result of declining emissions factors (i.e. emissions per unit energy production) over the western US (2021 values are normalized to 1). Panel C: total damages of the 2012-2016 drought in California, compared to estimates of the direct economic impacts from prior literature due to reductions in hydropower and the increased electricity demand (*27*, *28*). CO_2 damages are calculated using two SCC values, \$117 per ton as in panel A and \$193 per ton (under a 2% discount rate following (*43*)). In Panel C, we only calculate the impacts originating from fossil fuel plants in CA and impacts in other regions due to the runoff changes in CA.

generation come from CO_2 emissions (84% of total damage), while $PM_{2.5}$-related health damage and the CH_4 leakage each accounted for 10% and 6% of the total damage.

These monetized damages exceed the economic impacts of drought on the electricity system reported by previous studies (*27*, *28*). As a point of comparison, we focus on the 2012–2016 drought in California, a period which has been extensively studied. We account for the drought-induced damages associated with emissions from power plants in CA, as well as damages in the other two regions as a result of the CA drought. We estimate that the drought-induced CO_2 emissions account for 19% of the total electric CO_2 emissions in CA during this period (11% from CA plants,

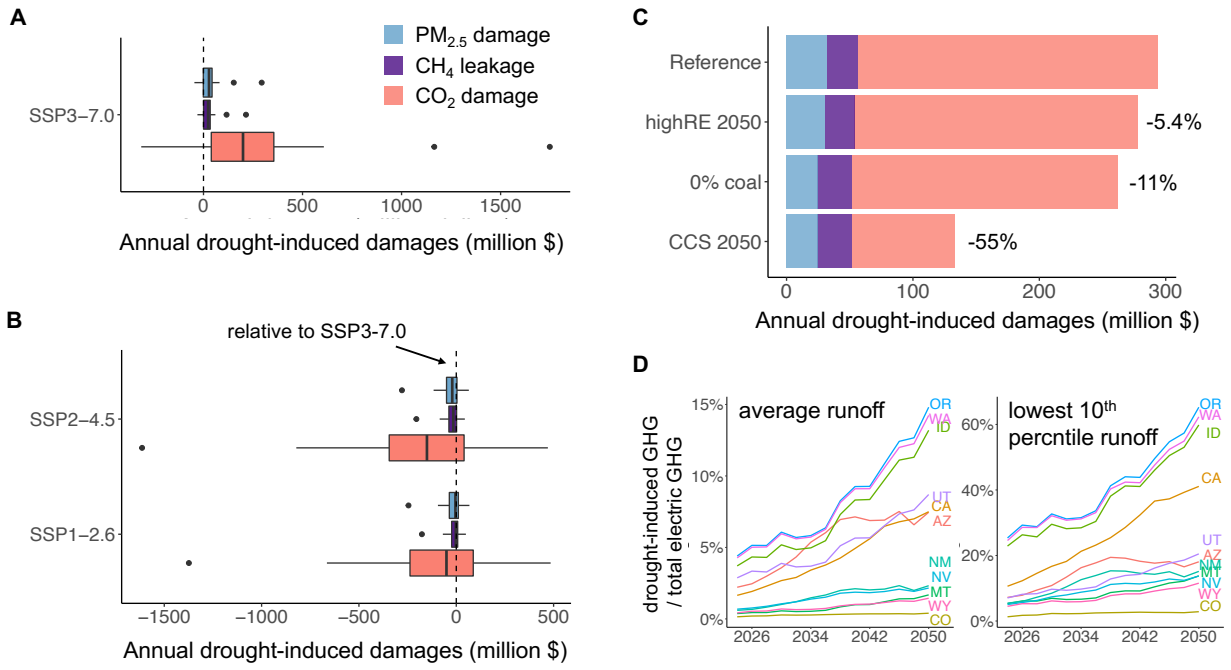

Figure 5: **Future damages of drought-induced fossil generation could be mitigated under low GHG scenarios and lower-carbon electricity sector scenarios.** Panel A: annual drought-induced damages projected by 33 climate models under the SSP3-7.0 scenario over 2030-2059 (relative to the 1980-2014 average of each model). Panel B: declines in monetized damages under low GHG scenarios (SSP1-2.6 and SSP2-4.5), relative to the SSP3-7.0 scenario. Panel C: projected electricity sector transitions reduce drought-induced damages at varying magnitudes (mean values of the 33 models under the SSP3-7.0). Panel D: increasing importance of the drought-induced GHG emissions relative to the total GHG emissions from the electricity sector, under the *high RE* scenario. GHG emissions included the CO_2 emissions and potential CH_4 leakages (aggregated using the global warming potential of 100 years). Drought-induced emissions are calculated using the average runoffs in 2030-2059 (left panel) or the 10th percentile lowest runoffs during 2030-2059 (right panel).

and 8% from the other two regions). The drought-induced fossil generation led to a total monetized damage of $5.1 billion (using SCC value of $117) — 1.2–1.9x of the reported direct economic cost due to the reduction in hydropower and 2.5x of the direct economic cost due to the drought-induced increase of electricity demand (*27*, *28*).

Projecting future damages

Despite the variability in projected runoffs across climate models, most models project increasing or sustaining drought risks (decreasing runoff) over the western US during 2030 to 2059 relative to 1980

to 2014 (see figure S13). Averaged across climate model projections under the reference scenario, drought-induced fossil fuel generation could result in annual damages of $293 million (relative to 1980-2014 averages of each model, discounted back to 2020). Damages due to extra CO_2 emissions accounts for 81% of the total damages, while CH_4 leakages and $PM_{2.5}$ damages account for 8% and 11%, respectively.

These drought-induced economic and health damages, however, could be substantially lower under the alternative climate scenarios with lower GHG emissions (SSP1-2.6 and SSP2-4.5). Compared to SSP3-7.0, we estimate a reduction in annual damages by $214 million under SSP2-4.5, or 73% of the damages under SSP3-7.0. This reduction is primarily driven by the higher projected runoff (less severe droughts) in California and Northwest projected by models under the two lower GHG scenarios. We find that the damages under SSP2-4.5 scenario are lower than the SSP1-2.6 scenario, likely due to the non-linear relationship between runoffs and the GHG forcings and model uncertainties. Runoff generally decreases under higher air temperature due to the increased evapotranspiration (*23*, *46*), but the substantial uncertainty in precipitation variability and the role of vegetation further complicates the runoff responses across different climate scenarios (*47*, *48*).

Surprisingly, the projected transitions in the electricity sector have modest effects in mitigating the damages from the drought-induced fossil generation, with the only exception of expansive penetration of CCS in 2050 (see figure 5C for the result of 2050, and figure S15 for the result of 2035). Relative to the reference scenario under SSP3-7.0, replacing all coal power plants with natural gas plants only reduces the drought-induced damages by 11%. Increased penetration of renewable energy and energy storage has an even smaller impact – a reduction in the damages by 5.4% in 2050. These modest effects are in sharp contrast with the total emission mitigations that could be achieved under these two strategies. Total CO_2 emissions from the fossil fuel plants would decline by 72% under NREL's *high RE* scenarios and by 26% under the *coal-phase out* scenario, respectively. These disparities are due to the underlying differences between the projected changes in *marginal* generators and *average* generators in the future (see figure S14). For example, fossil fuel generators are projected to only generate 8.6% of the total electricity in California in 2050 (compared to 41% in 2021), while they are still projected to be the dominant marginal generators, serving as the marginal generator in the grid for 71% of the time of a year. As a result of the differential changes between the average and marginal generators, we estimate that the relative contributions of drought-induced GHG emissions will increase by 2-4 fold in many western states over the next 30 years with increasing expansions of renewable energy (see figure 5D). For example,

drought-induced GHG emissions of California associated with an extreme drought year (defined as the 10th percentile lowest runoffs during 2030-2059) would account for 41% of the total electricity GHG emissions of California in 2050 (compared to only 11% in 2024).

Discussion

By empirically linking runoff variability to plant-level generation, emissions, and surface $PM_{2.5}$, our analysis quantifies the environmental and economic impacts associated with drought-induced fossil fuel generation. In the states that heavily rely on hydropower for electricity generation, drought-induced GHG emissions could account for up to 40% of the total electricity emissions of those states during future extreme drought years. Focusing on the 2012-2016 CA drought, we quantify that the monetized economic and health damages of the drought-induced fossil generation are 1.2-2.5x the previously reported economic costs of drought. Our analysis thus suggests that the impacts of drought on the electricity system have been underestimated by previous research that largely focuses on the economic costs of the drought-induced disruptions to the electricity sector.

We find that over 50% of the drought-induced fossil fuel generation - and the resulting economic and health damages - are trans-boundary. Through the interconnected electric grid, droughts in one region lead to increases in fossil fuel emissions in the neighboring regions. Our analysis thus further contributes to an emerging literature that evaluates the impacts of climate change on the electricity system through grid interconnections (which have mostly focused on the impacts on electricity prices and grid stability using power system models) (*19*, *26*). Previous studies have shown that the interregional connection could mitigate drought-induced risks in terms of grid stability and generation cost (*19*). Our analysis however demonstrates that the drought-induced emissions impacts could be re-distributed through the grid interconnection (consistent with findings from prior work (*30*)). More broadly, our results have important implications for research that uses empirical or statistical models to quantify the impacts of climate or other environmental change. Despite an emerging interest in the *transboundary* impacts of climate change through various interconnecting networks, many empirical studies focus on quantifying how *local* changes in climate affect local outcomes, such as energy expenditures, economic growth, or crop yields. Our analysis suggests that, at least in some settings, local economic impacts could be driven by distant climate change, and that a careful empirical strategy is needed to uncover these teleconnections.

Drought-induced economic and health damages from fossil fuel generation will remain an im-

portant challenge under future climate, as climate models project increased drought risks in many locations under a warming climate without timely GHG reductions, including the western US. However, these damages could be substantially reduced under mitigation scenarios which limit the warming level. Surprisingly, we find that increased penetration of renewable energy has little effect in reducing the drought-induced damages despite a significant reduction in the total fossil fuel generation under the evaluated scenario. This is largely because the amount of renewable energy projected to be deployed under the NREL scenario displaces a significant fraction of fossil fuel generation on average, but is not yet sufficient to fully replace them as the marginal generators. The drought-induced fossil fuel generation and associated damages will become increasingly important with the overall grid decarbonization, as the ratio of drought-induced fossil fuel generation to total fossil fuel generation gets larger. In other words, the electricity sector will become harder to be "fully decarbonized" if we account for the increasingly frequent drought shocks and the associated GHG emissions in systems with at least some hydro. Our research suggests that accounting for the impacts of climate change and its variability on the electricity system is important for decarbonization in the western US; such factors have been studied in some scenario analyses (*49*, *50*) but not fully integrated in most net-zero scenarios. More aggressive expansions of renewable energy and/or increased penetration of long-duration energy storage technology will likely further help mitigate the drought-induced damages we uncover.

Our research is, to our knowledge, the first to empirically quantify the impacts of drought-induced generation from fossil fuel plants on air quality. We show that drought conditions could further exacerbate ambient $PM_{2.5}$ pollution, a leading environmental risk factor around the world, through heavier usages of fossil fuels in the electricity system. More broadly, our analysis contributes to a better quantification of the impacts of climate change on human health through climate-induced changes in air pollution. Our work contributes to an emerging literature that climate change could influence air quality through influencing fossil energy usage (*51*), extending the focus beyond the impacts on naturally-induced emissions (such as through wildfire or precursors of ozone) or the chemistry/meteorology channels (*52*–*55*).

From the methodological perspective, our analysis contributes important insights to the measurement of air quality impacts of emission changes associated with environmental shocks or policies. We find our empirical estimates of the impacts on surface $PM_{2.5}$ differ from the results simulated with a reduced-complexity air quality model, InMAP, in many important ways. Our empirical method estimates a larger response of $PM_{2.5}$ to precursor emission changes near the fossil fuel plants, but

virtually no effect outside the 200 km radius (consistent with prior empirical analysis (45)). Our empirical estimates are consistent with previous studies that show InMAP underestimates the $PM_{2.5}$ concentration (or the $PM_{2.5}$-emission sensitivities) in the western US either comparing to the surface $PM_{2.5}$ monitors (56) or the full-complexity chemical transport model (57). More research is needed to better understand the strengths and limitations of estimating impacts of emissions changes on air quality with both the empirical method as well as process-based air quality models.

Our research reveals multiple pathways for future research to better understand the impacts of drought on the energy systems and the downstream impacts. In this work, we use the cumulative runoff in the previous 9 months to characterize drought conditions as it is more directly related to hydropower (compared to standard drought indices such as Palmer Drought Severity Index (58)). Therefore, our analysis is designed to capture the relatively longer-term impacts of the "hydrological droughts" on the electricity system. As the long-term runoff changes only partially relate to the temperature variations, our analysis therefore only partially captures the effects of the accompanying heatwaves on electricity demand and the associated generation from fossil fuel plants. Future studies could build on our empirical framework to directly incorporate the influence of heatwaves. Further, we only quantify the impacts on the fossil fuel plants that are connected to the grid due to the data availability. However, drought-induced decreases in hydropower could also increase the usage of back-up generators that are not connected to the grid, as well as non-electricity energy sources especially in other parts of the world (59). Future research could also benefit from projections that combine our empirical estimates, while accounting for more realistic policy scenarios and energy system constraints.

While our study has focused on the western US, our method and findings are globally relevant as many countries that heavily rely on hydro power have experienced increasing drought risk due to climate change. Globally, we identify 19 countries that are potentially vulnerable to drought-induced shocks to their electricity and energy system (see figure S16), primarily located in Central and South America, Africa, and South East Asia. These countries heavily depend on hydropower for their electricity generation (>15% of the annual electricity generation), and could potentially experience increasing drought risks as projected by the climate models (>5% decline in the average 2030-2059 runoff, the median across different climate models). For example, Honduras relies on hydropower to provide 53% of the nation's electricity and is projected to experience a 20% decrease in runoff by mid-century under SSP3-7.0. Electricity systems in many countries could be much more polluting compared to western US (with a more coal-dominant grid) and could therefore lead

to substantially higher economic and health damages due to deteriorated air quality and GHG emissions (*60*, *61*). Furthermore, drought-induced reductions of hydropower could result in black outs in countries that do not have enough excess electricity generating capacities, leading to further economic or health consequences (*62*, *63*). Better understanding drought-related impacts to the energy systems and consequent environmental and economic damages in a global sample of countries is an important avenue for future research.

Materials and Methods

Unit-level generation and emissions data

Our analysis focuses on the western US which spans three Energy Information Agency (EIA) electricity regions: California (CA), Northwest (NW), and Southwest (SW) (*38*). Hourly level electricity generation and emissions (CO_2, SO_2, and NO_x) of major fossil fuel electricity generating units (nameplate capacity >25 MW) are obtained from the EPA Air Market Program Data from 2001 to 2021 (*64*). We aggregate hourly emissions and generation to monthly level for each unit. Unit-level characteristics such as location, primary fuel type, and stack height are derived from the EPA Emissions & Generation Resource Integrated Database (*65*). In our main analysis, we only include an observation (i.e. unit-month) if the unit has operated or reported for more than three days during the month (see SI for more details on the sample restrictions). Our final sample consists of 95608 unit-months from 681 electricity generating units – 586 units that use natural gas, 91 units that use coal, and 4 units that use biomass or other fuel types. Our final sample covers 93% of electricity generation from fossil fuel plants (including biomass), and 50% of the total generation in the western US in 2019 (*65*).

Drought characterization

Following Herrera-Estrada et al. (*30*), we use the total runoff (sum of surface and subsurface runoffs) to characterize drought conditions. Previous studies have shown that runoff more accurately captures hydrological droughts and the influence on hydropower compared to other standardized drought indices (e.g. the Palmer Drought Severity Index) (*30*, *66*). We use monthly runoff data from the phase 2 of the North American Land Data Assimilation System (NLDAS-2) (*67*). In our main analysis, we use runoff values from the VIC land-surface model following recommendations from prior literature which suggest that the VIC model outperforms the other NLDAS-2 models (*68*). For each electricity region, we first calculate the state-level runoff averaged over grid cells in each state, and then calculate the regional runoff as a weighted average of state-level runoff (weighted by the state-level hydropower capacity). To capture the long-term dynamics of hydrological droughts, we calculate the running average of runoff for the previous 3-12 months and the monthly anomalies for different averaging windows. The runoff anomalies are calculated as the relative differences between the observed value and the 1980-2021 average runoff for each region and month. We use the 9-month

runoff anomalies in our main analysis and find largely consistent results when using runoff values calculated with different averaging windows and runoff from the other NLDAS-2 models (Noah and Mosaic) (see figure S1).

Empirical strategy: impacts of drought on fossil fuel generation

We estimate the following regression to quantify the impacts of drought on electricity generation from fossil fuel units, while accounting for the cross-regional impacts:

$$y_{igym} = \sum_{k \in \{CA,NW,SW\}} \{\beta_{gk} Q_{kym}\} + \gamma_g \boldsymbol{X_{igym}} + \eta_g y + \psi_{gm} + \theta_i + \epsilon_{igym} \quad (1)$$

where y_{igym} denotes the log of electricity generation from unit i in electricity region g, year y, and month-of-year m. Q_{kym} denotes the runoff anomalies of region k in year y, and month-of-year m. Separate equations are estimated for each electricity region g ($g \in \{CA, NW, SW\}$). β_{gk} are the parameters of main interest here, which estimate the causal impacts of change in runoff anomalies in region k on the generation from fossil fuel units in region g, conditional on the runoff anomalies in the other two regions. $\boldsymbol{X_{igym}}$ denotes the regional- and unit-level variables including monthly sales in electricity (i.e. electricity demand), generation of wind power and solar power, and the monthly average air temperature at the plant location. When estimating impacts of drought on fossil generation in the same region ($g = k$), $\boldsymbol{X_{igym}}$ captures possible mechanisms through which runoff could influence fossil generation, and therefore in our main analysis we report estimates without control variables (see below for the mechanism analysis). While estimating drought impacts on generation from the neighboring regions ($g \neq k$), we report estimates with these variables as controls, as they are not likely to represent the underlying mechanisms.

Our main specification includes linear year trend, month-of-year fixed effects, and unit-level fixed effects to control for the underlying trend and seasonality in fossil generation and runoff, as well as the time-invariant unobserved factors at the unit level. ϵ_{igym} represents the error term. β_{gk} are estimated using the weighted ordinary least square approach, weighted by the unit-level monthly average generation to estimate the impacts on total generation. Standard errors of the regression coefficients are clustered at the plant level. See SI for more details on the alternative specifications of the regression models.

To account for the heterogeneous impacts of drought on different fossil fuel plants, we further estimate equation 1 at the Balancing Authority (BA) × fuel type level. We separately estimate the regression equations for each group of power plants with the same fuel type in the same BA region. In total, we estimate 54 equations for the 54 BA-fuel subgroups. Resolving the impacts of drought on plant generation at a more dis-aggregated level is important for the air quality and health impact analysis, as one unit of emissions could have different impacts on human health depending on their proximity to population centers. For a small number of units (11 out of 681 units), we use the pooled regression coefficients at the regional level instead of the highly uncertain coefficients estimated at the BA-fuel level. (For these 11 units, the estimated displaced generation would exceed their total generation if we use the coefficients from the BA-fuel regressions.) The aggregated impacts on electricity generation are consistent across the regressions at the regional or the BA-fuel level (see figure S5).

Mechanisms of drought impacts on power plants: causal mediation analysis

We use causal mediation analysis to identify the mechanisms through which runoff changes impact the electricity generation from the fossil fuel plants. For the mediation analysis, we only focus on the drought impacts on fossil fuel plants in the same electricity region (i.e. the local effect), and only focus on CA and NW where the estimated local impacts are substantial. Mechanism analysis on the cross-boundary impacts are discussed in a separate section in the SI addressing the changes in the import/export of electricity. Causal mediation analysis is a widely used statistical technique across many disciplines that aims to estimate the causal effects of the treatment variable (in our case, runoff) on the outcome variable (in our case, fossil plant generation) through certain causal mechanisms (*69*). We focus on the following four pathways through which droughts could influence electricity generation from fossil fuel plants: 1) through changes in the hydropower output, 2) through changes in the electricity demand, 3) through changes in wind or solar power production, and 4) through changes in the cooling efficiency of thermal power plants due to ambient temperature. To estimate the effect through each mechanism (mediator variable), we first establish the relationship between runoff and the mediator variables (e.g., how runoff influences hydropower generation) and then estimate how runoff and the mediator variable could jointly influence fossil fuel generation. More details of the causal mediation analysis can be found in the SI.

Air quality impacts

We estimate an empirical model between predicted drought-induced fossil plant emissions and surface $PM_{2.5}$ concentration measured by monitors nearby. Using our estimates from the first part of the analysis, we first calculate the predicted drought-induced CO_2, SO_2, and NO_x emission changes at each plant using the following equation:

$$\Delta Emis_{iym} = \sum_{k \in \{CA,NW,SW\}} (e^{(\beta_{ki} \times Q_{kym})} - 1) \times Emis_{iym} \quad (2)$$

where $\Delta Emis_{iym}$ denotes drought-induced emissions for unit i in year y and month-of-year m. Q_{kym} denotes the monthly runoff anomaly of electricity region k. β_{ki} denotes the coefficients derived from the BA-fuel level regressions which estimates the impacts of runoff change in region k on unit i. $Emis_{iym}$ denotes the observed emissions from unit i in that month. $\Delta Emis_{iym}$ quantifies the changes in emissions due to runoff anomalies relative to a counterfactual scenario that the monthly runoff is the same as the 1980-2021 average. $\Delta Emis_{iym}$ could be both positive (when runoff is lower than the 1980-2021 average) or negative (when runoff is higher).

Surface $PM_{2.5}$ concentrations are derived from the US Air Quality Systems administered by the US EPA (*70*). Due to influences of drought on wildfire and associated $PM_{2.5}$ concentration (*53*, *55*), we only use observational $PM_{2.5}$ concentration from monitors on days that are not influenced by wildfire smoke using methods from (*71*) (see SI for more details). We calculate the monthly-average $PM_{2.5}$ concentration for each month and monitor using $PM_{2.5}$ concentration on all non-smoke days. Our air quality analysis focuses on the period between 2006 and 2020 due to the availability of the wildfire smoke plume data.

We estimate the following regression to quantify the effects of drought-induced emissions on surface $PM_{2.5}$ concentration:

$$PM_{iym} = \sum_{d} \beta_d \Delta Emis_{idym} + \gamma \boldsymbol{W_{iym}} + \eta_y + \psi_m + \theta_i + \epsilon_{iym} \quad (3)$$

where PM_{iym} denotes the monthly non-smoke $PM_{2.5}$ concentration measured by monitor i on year y, month-of-year m. $\Delta Emis_{idym}$ is the drought-induced emission changes (SO_2 + NO_x) from fossil fuel plants that are located within a certain distance (distance bin d) from the monitor i. For each monitor, fossil fuel plants are grouped into five groups based on their distances from the monitors: *<50 km, 50-100km, 100-200km, 200-500km, >500km.* $\boldsymbol{W_{iym}}$ are the meteorological variables at

the location of monitor i. In our main specification, we include the splines of surface temperature, precipitation, dewpoint temperature, boundary layer height, air pressure, 10m wind direction (U and V components) and wind speed. Our main specification includes year (η_y) and month-of-year fixed effects (ψ_m) to capture the interannual variability and seasonality of $PM_{2.5}$ concentration, and monitor-level fixed effects (θ_i) to control for the time-invarying unobserved factors at the monitor level. ϵ_{iym} represents the error term. β_d are estimated using the weighted ordinary least square approach, weighted by the variance of the inversely distance-weighted drought-induced emissions of each monitor to reduce the uncertainty of the estimates (i.e. observations from monitors are up-weighted if the monitors are closer to plants with substantial changes in drought-induced emissions). Standard errors of the regression coefficients are clustered at the state×year×month level.

To better understand if the estimated impacts capture the causal impacts of emission changes on surface $PM_{2.5}$, we further divide the drought-induced emissions (from a given distance bin) into three categories depending on wind direction and the location of fossil fuel plants and air quality monitors. Following methods in (*72*), drought-induced emissions are classified into "upwind" or "downwind", depending on whether the fossil fuel plants are at the upwind or downwind direction of the monitor. We find the drought-induced emissions from upwind power plants have a larger impact on surface $PM_{2.5}$ compared to emissions from the downwind power plants, although estimates are somewhat noisy (see figure S7).

As an alternative strategy to model the air quality impacts, we also use the Intervention Model for Air Pollution (InMAP) to calculate the impacts of drought-induced emissions of SO_2 and NO_x on $PM_{2.5}$ concentrations. More details of the InMAP simulations could be found in SI.

Health impacts analysis

We quantify the health impacts of drought-induced fossil fuel generation in terms of the premature mortality associated with changes in $PM_{2.5}$. As we calculate $PM_{2.5}$ changes at the monthly level due to the runoff variability, we use the concentration response function (CRF) between mortality and short-term exposure of $PM_{2.5}$ (e.g., at the daily or weekly level), rather than CRFs derived from long-term epidemiological studies. In our main analysis, we use the CRF from Deryugina et al. to quantify the premature mortalities for adults over 65 years old (*32*). Deryugina et al. estimate that every 1 $\mu g/m^3$ increase of $PM_{2.5}$ at the daily level leads to an increase of 0.69 deaths per million people in the following three days for adults over 65 years old in the US. Their study exploits the variation of daily $PM_{2.5}$ due to daily wind direction changes, and shows that the estimated impacts

of $PM_{2.5}$ on mortality are substantially higher compared to methods that do not fully account for the confounding biases. We calculate the premature mortality among the 65+ age population at the monthly and census tract-level associated with drought-induced changes of $PM_{2.5}$. Population information of different age groups is derived from the 5-year American Community Survey (ACS) data during 2006-2010 (*73*). The health impacts are monetized using a value of statistical life (VSL) of $10.95 million (year 2019 dollars), as recommended by the US EPA (*33*) and used in previous studies (*74*). While we use the main estimate of the three-day window from (*32*) in our main analysis - as we believe its empirical approach carefully accounts for the confounding biases - we also calculate the health impacts on premature mortality using alternative CRFs from (*75*–*77*) and alternative estimates from (*32*) using different time windows (see figure S10).

Projecting future impacts

We assess potential impacts of future drought on emissions and air quality under future climate and electricity sector scenarios (scenarios detailed below). We select the year 2035 and 2050 as our projection points to capture both the potential near-term and medium-term energy transitions. We project the future drought-induced electricity generation and emissions (CO_2, NO_x, and SO_2) from fossil fuel plants that are still in operation in 2021.

Future damages are calculated using SCC, SC-CH_4, and VSL adjusted for future climate damages and income growth. These future damages are then discounted back to year 2020 using a discount rate of 2.5%. For SCC, we use the values of 158$ per ton (emissions year 2035) and 205$ per ton (emissions year 2050). For SC-CH_4, we use the values of 2313$ per ton (emissions year 2035) and 3547$ per ton (emissions year 2050). Both values are derived from the latest US EPA report, calculated using a 2.5% discount rate (*34*). For the air quality impacts, we use the empirical relationship between surface $PM_{2.5}$ and drought-induced emissions and project the mortalities using CRFs from (*32*) and future projected population for the 65+ age group (*78*). For VSL, we follow a similar method from Carleton et al. (*74*) to calculate the future VSL values using the projected economic growth in the US from OECD-ENV model under the SSP3 scenario (*79*) and income elasticity of one.

Future electricity sector scenarios

For the electricity sector scenarios, we construct highly stylized scenarios to quantify the impacts of future drought under potential changes in the electricity sector (Table 1). These scenarios are

Table 1: Electricity sector scenarios.

Scenarios	**2035**	**2050**
Reference	using the displacement pattern from the empirical model.	
Coal phase-outs	50% coal replaced by average gas plants	100% coal replaced by average gas plants
CCS penetration	10.7% gas generation with CCS (removal rate: 90%)	68.5% gas generation with CCS (removal rate: 90%)
High RE	calculating emission changes using %hours of fossil energy on the margin (derived from the NREL hourly simulation results).	

Note: *Coal phase-out* scenarios assume that the coal power plants are replaced by natural gas plants in the same location. *CCS penetration* sceanrios assume that some natural gas plants are retrofitted with CCS on top of the *coal phase-out* scenario. The penetration and removal rate of CCS is derived from the Princeton Net Zero America study (*37*). *High RE* scenario uses the hourly simulation outputs from the Cambium data from the National Renewable Energy Laboratory (*36*), which simulates the marginal energy source for each hour for each Balancing Area.

not designed to correspond to any current or proposed policies, but rather to reflect potential comparative changes in the electricity system.

We examine the following scenarios: 1) the *reference* scenario which assumes no changes in the electricity sector; 2) the *coal phase-out* scenario which assumes a partial or full phase-out of coal power plants in the electricity grid and retired coal plants are replaced by new natural gas plants; 3) the *CCS penetration* scenario which assumes that some natural gas plants are retrofitted with CCS **on top of** the *coal phase-out* scenario; and 4) the *high RE* scenario which examines the impacts of expanding renewable energy sources on the marginal energy sources used for electricity generation and the associated drought-induced emissions. For the *coal phase-out* scenario, we assume 50% of the coal generation in 2035, and 100% of the coal generation in 2050 is replaced by natural gas plants with average emission factors within each region. For the *CCS* scenario, we use the modeling results from the Princeton Net Zero America study (*37*) which projects the amount of electricity generated using natural gas with and without the CCS technology. Averaged across their four scenarios (*E+, E-, E+RE-, E-B+*), 10.7% and 68.5% of the US gas electricity generation is projected to be generated by plants with CCS technology in 2035 and 2050, respectively.

For the *high RE* scenario, we use the hourly simulation outputs from the Cambium data from the National Renewable Energy Laboratory (*36*). As the model simulates the marginal energy source for each hour and each Balancing Area, we calculate the time percentage for which the fossil energy

is on the margin for each electricity region at the monthly, we assume that the drought-induced electricity gap will be solely provided by the non-fossil energy resulting in zero drought-induced emissions. We further design two cases for the *high RE* scenario, to further explore the potential impacts of expanded RE on the interregional exchange of electricity and its implications on the drought-induced impacts (see SI).

Future climate change scenarios

For future climate change scenarios, we use the projected runoff values (surface + subsurface) from the Coupled Model Intercomparison Project Phase 6 (CMIP6). We examine three primary climate forcing scenarios featured by the IPCC, which constructed as pairs between the Shared Socio-economic Pathways (SSPs) and the Representative Concentration Pathways (RCPs) (*80*). We use SSP1-2.6 (which the IPCC refers to as the "Low" scenario), SSP2-4.5 (which the IPCC refers to as the "Intermediate" scenario), and SSP3-7.0 (which the IPCC refers to as the "High" scenario). We use projections from 33 global climate models with available runoff output at the monthly level for the historical and three climate scenarios (table S2). Only one ensemble variant is selected for each model – we use the first ensemble variant of each model ("r1i1p1f1") when possible and use the other ensemble variants if "r1i1p1f1" is not available. To be consistent with our empirical analysis, for each climate model realization, we first calculate the regional monthly runoff values by taking the weighted average of the state-level runoff weighted by the hydropower capacity (capacity is fixed at the 2021 level). We then calculate the 9-month moving average values for each region and calculate the monthly anomalies relative to the monthly averages derived from the historical simulation (1980-2014) of each model. We use the average runoff anomalies from 2030 to 2059, for each climate model and climate scenario.

Acknowledgments

We thank Brandon de la Cuesta for helpful discussions on the mediation analysis. We thank Carlos F. Gould, Jessica Li, and members of Stanford ECHOLab and Center on Food Security and the Environment for helpful comments. Some of the computing for this project was performed on the Stanford Sherlock cluster, and we would like to thank Stanford University and the Stanford Research Computing Center for providing computational resources and support that contributed to these research results. MQ acknowledges the support from the planetary health fellowship at Stanford's Center for Innovation in Global Health.

Author contributions

All authors contributed to the conception and design of the study. MQ led the data analysis and impacts modeling with inputs from all authors. MQ and MB led the writing of the manuscript with inputs from all authors.

Competing interests

The authors declare no competing interests.

Data and materials availability

All data and code will be made available on a public repo upon publication

References

1. H.-O. Pörtner, D. C. Roberts, *et al.*, Climate change 2022: Impacts, adaptation and vulnerability. (2022).

2. R. Schaeffer *et al.*, Energy sector vulnerability to climate change: A review. *Energy* **38**, 1–12 (2012).

3. M. T. Van Vliet, D. Wiberg, S. Leduc, K. Riahi, Power-generation system vulnerability and adaptation to changes in climate and water resources. *Nature Climate Change* **6**, 375–380 (2016).

4. J. Cronin, G. Anandarajah, O. Dessens, Climate change impacts on the energy system: a review of trends and gaps. *Climatic change* **151**, 79–93 (2018).

5. D. M. Ward, The effect of weather on grid systems and the reliability of electricity supply. *Climatic Change* **121**, 103–113 (2013).

6. M. Auffhammer, P. Baylis, C. H. Hausman, Climate change is projected to have severe impacts on the frequency and intensity of peak electricity demand across the United States. *Proceedings of the National Academy of Sciences* **114**, 1886–1891 (2017).

7. A. Rode *et al.*, Estimating a social cost of carbon for global energy consumption. *Nature* **598**, 308–314 (2021).

8. M. D. Bartos, M. V. Chester, Impacts of climate change on electric power supply in the Western United States. *Nature Climate Change* **5**, 748–752 (2015).

9. M. T. Van Vliet, J. Sheffield, D. Wiberg, E. F. Wood, Impacts of recent drought and warm years on water resources and electricity supply worldwide. *Environmental Research Letters* **11**, 124021 (2016).

10. I. Tobin *et al.*, Vulnerabilities and resilience of European power generation to 1.5 C, 2 C and 3 C warming. *Environmental Research Letters* **13**, 044024 (2018).

11. E. D. Coffel, J. S. Mankin, Thermal power generation is disadvantaged in a warming world. *Environmental Research Letters* **16**, 024043 (2021).

12. S. G. Yalew *et al.*, Impacts of climate change on energy systems in global and regional scenarios. *Nature Energy* **5**, 794–802 (2020).

13. W. Wan, J. Zhao, E. Popat, C. Herbert, P. Döll, Analyzing the Impact of Streamflow Drought on Hydroelectricity Production: A Global-Scale Study. *Water Resources Research* **57**, e2020WR028087 (2021).

14. E. A. Byers, G. Coxon, J. Freer, J. W. Hall, Drought and climate change impacts on cooling water shortages and electricity prices in Great Britain. *Nature communications* **11**, 1–12 (2020).

15. S. W. Turner, N. Voisin, J. Fazio, D. Hua, M. Jourabchi, Compound climate events transform electrical power shortfall risk in the Pacific Northwest. *Nature communications* **10**, 1–8 (2019).

16. D. L. Donaldson, D. M. Piper, D. Jayaweera, Temporal solar photovoltaic generation capacity reduction from wildfire smoke. *IEEE Access* **9**, 79841–79852 (2021).

17. F. Petrakopoulou, A. Robinson, M. Olmeda-Delgado, Impact of climate change on fossil fuel power-plant efficiency and water use. *Journal of Cleaner Production* **273**, 122816 (2020).

18. P. L. Joskow, California's electricity crisis. *oxford review of Economic Policy* **17**, 365–388 (2001).

19. N. Voisin *et al.*, Impact of climate change on water availability and its propagation through the Western US power grid. *Applied Energy* **276**, 115467 (2020).

20. N. S. Diffenbaugh, D. L. Swain, D. Touma, Anthropogenic warming has increased drought risk in California. *Proceedings of the National Academy of Sciences* **112**, 3931–3936 (2015).

21. A. P. Williams *et al.*, Large contribution from anthropogenic warming to an emerging North American megadrought. *Science* **368**, 314–318 (2020).

22. U.S. Environmental Protection Agency, *Emissions and Generation Resource Integrated Database (eGRID) 2019*, 2019.

23. B. Cook *et al.*, Twenty-first century drought projections in the CMIP6 forcing scenarios. *Earth's Future* **8**, e2019EF001461 (2020).

24. J. Lund, J. Medellin-Azuara, J. Durand, K. Stone, Lessons from California's 2012–2016 drought. *Journal of Water Resources Planning and Management* **144**, 04018067 (2018).

25. Y. Su, J. D. Kern, P. M. Reed, G. W. Characklis, Compound hydrometeorological extremes across multiple timescales drive volatility in California electricity market prices and emissions. *Applied Energy* **276**, 115541 (2020).

26. J. Hill, J. Kern, D. E. Rupp, N. Voisin, G. Characklis, The effects of climate change on inter-regional electricity market dynamics on the US West Coast. *Earth's Future* **9**, e2021EF002400 (2021).

27. J. D. Kern, Y. Su, J. Hill, A retrospective study of the 2012–2016 California drought and its impacts on the power sector. *Environmental Research Letters* **15**, 094008 (2020).

28. P. H. Gleick, Impacts of California's ongoing drought: hydroelectricity generation. *Oakland, Calif.: Pacific Institute. Retrieved January* **21**, 2016 (2015).

29. E Hardin *et al.*, California drought increases CO2 footprint of energy. *Sustainable cities and society* **28**, 450–452 (2017).

30. J. E. Herrera-Estrada, N. S. Diffenbaugh, F. Wagner, A. Craft, J. Sheffield, Response of electricity sector air pollution emissions to drought conditions in the western United States. *Environmental Research Letters* **13**, 124032 (2018).

31. J. Eyer, C. J. Wichman, Does water scarcity shift the electricity generation mix toward fossil fuels? Empirical evidence from the United States. *Journal of Environmental Economics and Management* **87**, 224–241 (2018).

32. T. Deryugina, G. Heutel, N. H. Miller, D. Molitor, J. Reif, The mortality and medical costs of air pollution: Evidence from changes in wind direction. *American Economic Review* **109**, 4178–4219 (2019).

33. U.S. Environmental Protection Agency, *Regulatory Impact Analysis for the Clean Power Plan Final Rule*, 2015.

34. U. E. P. Agency, *Report on the Social Cost of Greenhouse Gases: Estimates Incorporating Recent Scientific Advances*, 2022.

35. T. A. Deetjen, I. L. Azevedo, Climate and health benefits of rapid coal-to-gas fuel switching in the US power sector offset methane leakage and production cost increases. *Environmental Science & Technology* **54**, 11494–11505 (2020).

36. P. Gagnon, W. Frazier, W. Cole, E. Hale, "Cambium Documentation: Version 2021", tech. rep. (National Renewable Energy Lab.(NREL), Golden, CO (United States), 2021).

37. E. Larson *et al.*, "Net-Zero America: Potential Pathways, Infrastructure, and Impacts, Final report", tech. rep. (Princeton University, Princeton, NJ, 2020).

38. U.S. Energy Information Administration, *Hourly Electric Grid Monitor*, 2021.

39. T. W. Juliano *et al.*, Smoke from 2020 United States wildfires responsible for substantial solar energy forecast errors. *Environmental Research Letters* **17**, 034010 (2022).

40. S. D. Gilletly, N. D. Jackson, A. Staid, presented at the 2021 IEEE 48th Photovoltaic Specialists Conference (PVSC), pp. 1619–1625.

41. L. Lledó, O. Bellprat, F. J. Doblas-Reyes, A. Soret, Investigating the effects of Pacific sea surface temperatures on the wind drought of 2015 over the United States. *Journal of Geophysical Research: Atmospheres* **123**, 4837–4849 (2018).

42. C. W. Tessum, J. D. Hill, J. D. Marshall, InMAP: A model for air pollution interventions. *PloS one* **12**, e0176131 (2017).

43. T. Carleton, M. Greenstone, A guide to updating the US Government's social cost of carbon. *Review of Environmental Economics and Policy* **16**, 196–218 (2022).

44. J. A. De Gouw, D. D. Parrish, G. J. Frost, M. Trainer, Reduced emissions of CO2, NOx, and SO2 from US power plants owing to switch from coal to natural gas with combined cycle technology. *Earth's Future* **2**, 75–82 (2014).

45. J. A. Burney, The downstream air pollution impacts of the transition from coal to natural gas in the United States. *Nature Sustainability* **3**, 152–160 (2020).

46. D. Touma, M. Ashfaq, M. A. Nayak, S.-C. Kao, N. S. Diffenbaugh, A multi-model and multi-index evaluation of drought characteristics in the 21st century. *Journal of Hydrology* **526**, 196–207 (2015).

47. A. L. Swann, F. M. Hoffman, C. D. Koven, J. T. Randerson, Plant responses to increasing CO2 reduce estimates of climate impacts on drought severity. *Proceedings of the National Academy of Sciences* **113**, 10019–10024 (2016).

48. J. S. Mankin, R. Seager, J. E. Smerdon, B. I. Cook, A. P. Williams, Mid-latitude freshwater availability reduced by projected vegetation responses to climate change. *Nature Geoscience* **12**, 983–988 (2019).

49. A. Miara *et al.*, Climate-water adaptation for future US electricity infrastructure. *Environmental science & technology* **53**, 14029–14040 (2019).

50. J. Wessel, J. D. Kern, N. Voisin, K. Oikonomou, J. Haas, Technology pathways could help drive the US West Coast grid's exposure to hydrometeorological uncertainty. *Earth's Future*, e2021EF002187 (2022).

687 *51.* D. W. Abel *et al.*, Air-quality-related health impacts from climate change and from adaptation
688 of cooling demand for buildings in the eastern United States: An interdisciplinary modeling
689 study. *PLoS medicine* **15**, e1002599 (2018).

690 *52.* D. E. Horton, C. B. Skinner, D. Singh, N. S. Diffenbaugh, Occurrence and persistence of future
691 atmospheric stagnation events. *Nature climate change* **4**, 698–703 (2014).

692 *53.* Y. Wang *et al.*, Adverse effects of increasing drought on air quality via natural processes.
693 *Atmospheric Chemistry and Physics* **17**, 12827–12843 (2017).

694 *54.* P. Achakulwisut *et al.*, Effects of increasing aridity on ambient dust and public health in the
695 US Southwest under climate change. *GeoHealth* **3**, 127–144 (2019).

696 *55.* Y. Xie *et al.*, Tripling of western US particulate pollution from wildfires in a warming climate.
697 *Proceedings of the National Academy of Sciences* **119**, e2111372119 (2022).

698 *56.* A. L. Goodkind, C. W. Tessum, J. S. Coggins, J. D. Hill, J. D. Marshall, Fine-scale damage es-
699 timates of particulate matter air pollution reveal opportunities for location-specific mitigation
700 of emissions. *Proceedings of the National Academy of Sciences* **116**, 8775–8780 (2019).

701 *57.* M. Qiu, C. M. Zigler, N. E. Selin, Impacts of wind power on air quality, premature mortality,
702 and exposure disparities in the United States. *Science Advances* **8**, eabn8762, eprint: https:
703 //www.science.org/doi/pdf/10.1126/sciadv.abn8762 (2022).

704 *58.* J. Sheffield, E. F. Wood, M. L. Roderick, Little change in global drought over the past 60
705 years. *Nature* **491**, 435–438 (2012).

706 *59.* I. Ahmed, P. Parikh, G. Sianjase, D. Coffman, The impact decades-long dependence on hy-
707 dropower in El Niño impact-prone Zambia is having on carbon emissions through backup diesel
708 generation. *Environmental Research Letters* **15**, 124031 (2020).

709 *60.* J. Yang, Y. Huang, K. Takeuchi, Does drought increase carbon emissions? Evidence from
710 Southwestern China. *Ecological Economics* **201**, 107564 (2022).

711 *61.* N. Wu *et al.*, Daily Emission Patterns of Coal-Fired Power Plants in China Based on Multi-
712 source Data Fusion. *ACS Environmental Au* (2022).

713 *62.* M. A. Cole, R. J. Elliott, E. Strobl, Climate change, hydro-dependency, and the African dam
714 boom. *World Development* **60**, 84–98 (2014).

715 *63.* K. E. Gannon *et al.*, Business experience of floods and drought-related water and electricity
716 supply disruption in three cities in sub-Saharan Africa during the 2015/2016 El Niño. *Global*
717 *Sustainability* **1** (2018).

718 *64.* U.S. Environmental Protection Agency, *Air Markets Program Data (AMPD)*, 2021.

719 *65.* U.S. Environmental Protection Agency, *Emissions and Generation Resource Integrated Database*
720 *(eGRID) 2019*, 2019.

721 *66.* K. E. Trenberth *et al.*, Global warming and changes in drought. *Nature Climate Change* **4**,
722 17–22 (2014).

723 *67.* Y. Xia *et al.*, Continental-scale water and energy flux analysis and validation for the North
724 American Land Data Assimilation System project phase 2 (NLDAS-2): 1. Intercomparison and
725 application of model products. *Journal of Geophysical Research: Atmospheres* **117** (2012).

726 *68.* Y. Xia *et al.*, Continental-scale water and energy flux analysis and validation for North Amer-
727 ican Land Data Assimilation System project phase 2 (NLDAS-2): 2. Validation of model-
728 simulated streamflow. *Journal of Geophysical Research: Atmospheres* **117** (2012).

729 *69.* D. Tingley, T. Yamamoto, K. Hirose, L. Keele, K. Imai, Mediation: R package for causal
730 mediation analysis. (2014).

731 *70.* U.S. Environmental Protection Agency, *Air Data: Air Quality Data Collected at Outdoor Mon-*
732 *itors Across the US*, 2022.

733 *71.* M. L. Childs *et al.*, Daily Local-Level Estimates of Ambient Wildfire Smoke PM2. 5 for the
734 Contiguous US. *Environmental Science & Technology* (2022).

735 *72.* H. K. Pullabhotla, M. Zahid, S. Heft-Neal, V. Rathi, M. Burke, Global biomass fires and infant
736 mortality. (2022).

737 *73.* U.S. Census Bureau, *U.S. Population by Gender and Age groups (ACS 5-Year Estimates,*
738 *2006-2010)*, 2010.

739 *74.* T. Carleton *et al.*, Valuing the global mortality consequences of climate change accounting for
740 adaptation costs and benefits. *The Quarterly Journal of Economics* **137**, 2037–2105 (2022).

741 *75.* Q. Di *et al.*, Association of short-term exposure to air pollution with mortality in older adults.
742 *Jama* **318**, 2446–2456 (2017).

743 *76.* C. Liu *et al.*, Ambient particulate air pollution and daily mortality in 652 cities. *New England*
744 *Journal of Medicine* **381**, 705–715 (2019).

745 *77.* P. Orellano, J. Reynoso, N. Quaranta, A. Bardach, A. Ciapponi, Short-term exposure to par-
746 ticulate matter (PM10 and PM2. 5), nitrogen dioxide (NO2), and ozone (O3) and all-cause
747 and cause-specific mortality: Systematic review and meta-analysis. *Environment international*
748 **142**, 105876 (2020).

749 *78.* U.S. Census Bureau, *The 2017 National Population Projections*, 2018.

750 *79.* R. Dellink, J. Chateau, E. Lanzi, B. Magné, Long-term economic growth projections in the
751 Shared Socioeconomic Pathways. *Global Environmental Change* **42**, 200–214 (2017).

752 *80.* IPCC, in *Climate Change 2021: The Physical Science Basis. Contribution of Working Group I*
753 *to the Sixth Assessment Report of the Intergovernmental Panel on Climate Change*, ed. by V.
754 Masson-Delmotte *et al.* (Cambridge University Press, Cambridge, United Kingdom and New
755 York, NY, USA, 2021), 3−32.

756 *81.* S. L. Decker, Officials identify steam plant accident victim. *The Chronicle* (May 11, 2005).

Supplementary information

Drought impacts on the electricity system, emissions, and air quality in the western US

Minghao Qiu [a,b,1], Nathan Ratledge [c], Inés Azevedo [d], Noah S. Diffenbaugh [e], Marshall Burke [e,f,g],

a Department of Earth System Science, Stanford University, Stanford, CA, USA

b Center for Innovation in Global Health, Stanford University, Stanford, CA, USA

c Emmett Interdisciplinary Program in Environment and Resources, Stanford University, Stanford, CA, USA

d Department of Energy Science and Engineering, Stanford University, Stanford, CA, USA

e Doerr School of Sustainability, Stanford University, Stanford, CA, USA

f Center on Food Security and the Environment, Stanford University, Stanford, CA, USA

g National Bureau of Economic Research, Cambridge, MA, USA

1 To whom correspondence should be addressed. E-mail: mhqiu@stanford.edu

Supplementary methods

Alternative specifications of the regression models

To explore the robustness of our estimation results across model specifications, we conduct three sensitivity analysis to estimate the runoff impacts on electricity generation from fossil fuel plants:

1) **Estimating the regression models using alternative drought indices.** Our main analysis uses the 9-month average runoff anomalies computed from the NLDAS-2 VIC model. We also estimate the regression models using runoff anomalies averaged over different windows (3, 6, 9, and 12 months), as well as the runoff anomalies from the other NLDAS-2 models (Noah and Mosaic). We find largely consistent results when using alternative drought indices (see figure S1).

2) **Estimating the regression models using alternative model specifications.** Our main analysis includes monthly sales in electricity (i.e. electricity demand), generation of wind power and solar power, and the monthly average air temperature at the plant location as co-variates. The main specification also includes linear year trend, month-of-year fixed effects, and unit-level fixed effects to control for the underlying trend and seasonality in fossil generation and runoff, as well as the time-invariant unobserved factors at the unit level. Coefficients are estimated using the weighted ordinary least square approach, weighted by the unit-level monthly average generation. We further estimate regression models which do not include control variables ('No ctrl' in figure S2), models which include natural gas as additional control variable ('Ctrl+Gas price'), models which estimate the coefficients with ordinary least square ('Non-weighted'), models which include year fixed effects instead of linear year trend ('Year FE'), and models that specify a quadratic relationship between runoff anomalies and electricity generation. We find the estimation results are largely consistent across alternative specifications of the regression models (see figure S2).

3) **Estimating the regression models using alternative sample restrictions.** In our main analysis, we only include an observation (i.e. unit-month) if the unit has operated or reported for more than three days during the month. Figure S3 shows the estimation results across different samples which include an observation if the unit has operated or reported for more than X days during the month (X=1,..,10). As the sample becomes more restricted (i.e. X gets larger), the estimated impacts are likely less influenced by outliers (due to potential missing values). However, a more restricted sample might also fail to capture signals from marginal power plants that only operate a few days a month. Considering this trade off, our main analysis chooses X=4 as the

restriction criterion for our main analysis, as magnitudes of the estimated coefficients remain largely stable after X>3.

Interregional import and export of electricity

To further understand the trans-boundary impacts of runoff on fossil power plants, we use the hourly electricity import and export data from EIA to estimate how drought influences the inter-regional exchange of electricity between the three regions in the western US (*1*). Hourly electricity production, demand, and exchange between electric electricity regions are available since July 2015. Using data from 2016 to 2021, we estimate the following regression:

$$Export_{ym}^{i->j} = \beta_{ij} Q_{jym} + \gamma_g \boldsymbol{X_{iym}} + \theta_i Export_{ym}^{i->other} + \eta_{iy} + \psi_{im} + \epsilon_{iym}$$

where $\text{Export}_{ym}^{i->j}$ denotes the net export from electricity region i to electricity region j on year y and month-of-year m, Q_{jym} denotes the runoff anomalies of region j on year y month m. $\boldsymbol{X_{iym}}$ denotes a set of control variables, including the hydro generation, electricity demand, solar and wind generation of region i. $Export_{ym}^{i->other}$ denotes the export from region i to the other electricity region (other than j). η_{iy} and ψ_{im} denote year and month-of-year fixed effects. ϵ_{iym} is the normally-distributed error term. Here, the main coefficient of interest is β_{ij}, which quantify the impacts of runoff changes in region j on the net export of electricity from region i to j, conditional on the export to the other region and generation of region i.

Causal mediation analysis

We use causal mediation analysis to identify the mechanisms through which runoff changes impact the electricity generation from the fossil fuel plants. We focus on the following four mechanisms through which runoff changes could influence electricity generation from fossil fuel plants: 1) through changes in hydropower output (mediator variable: monthly hydropower generation), 2) through changes in electricity demand (mediator: monthly electricity demand), 3) through changes in wind or solar power production (mediator: monthly generation from solar and wind power), and 4) through changes in cooling efficiency of thermal power plants due to ambient temperature (mediator: average ambient temperature at the plant locations).

For the mediation analysis, we only focus on the drought impacts on the fossil fuel plants in the same electricity region (i.e. the local effect), and only focus on CA and NW where the estimated local effects are substantial. We use the R package "mediation" to perform the mediation analysis

(2). For each potential mediator M, we estimate the following *outcome model*:

$$y_{gym} = \beta_g^O Q_{gym} + \gamma_g M_{gym} + \lambda_g^O \boldsymbol{X_{gym}} + \eta_{gy} + \psi_{gm} + \epsilon_{gym} \tag{1}$$

and the following *mediator model*:

$$M_{gym} = \beta_g^M Q_{gym} + \lambda_g^M \boldsymbol{X_{gym}} + \eta_{gy} + \psi_{gm} + \epsilon_{gym} \tag{2}$$

where y_{gym} denotes the log of the total fossil generation in the electricity region g, year y, and month-of-year m. M_{gym} denotes the mediator variable. Q_{gym} denotes the runoff anomalies in electricity region g, year y. $\boldsymbol{X_{gym}}$ denote the control variables including runoff anomalies of the other two electricity regions and the other three mediators (except for M_{gym}). The *outcome model* (equation 1) thus estimates how runoff and the mediator jointly influence the fossil generation, conditioned on the other potential mechanisms and runoff in the neighboring regions. The *mediator model* (equation 2) estimates the relationship between mediator and the runoff, conditioned on the other potential mechanisms and runoff in the neighboring regions. The causal mediation effect (i.e. the causal effect runoff influence fossil fuel generation through mediator M) is then estimated by evaluating the changes in y_{gym} associated with changes in M due to changes in Q, while importantly, not through the direct impacts of Q on y as characterized by equation 1.

Air quality impacts: determining smoke day

Due to influences of drought on wildfire and associated $PM_{2.5}$ concentration (3, 4), we only use observational $PM_{2.5}$ concentration from monitors on days that are not influenced by wildfire smoke. Following the method from (5), we classify a day as a "smoke day" if the monitor location either has identified smoke plume overhead, or the monitor location intersects with modeled air particle trajectories from nearby fires when clouds may obscure plume identification. Smoke plume information is derived from the National Oceanic and Atmospheric Administration Hazard Mapping System, which provides analyst-identified plume boundaries based on visible bands of satellite imagery (6–8). Our air quality analysis focuses on the period between 2006 and 2020 due to the availability of the wildfire smoke plume data.

Alternative strategy to model the air quality impacts: InMAP

As an alternative strategy to model the air quality impacts, we also use the Intervention Model for Air Pollution (InMAP) to calculate the impacts of drought-induced emissions of SO_2 and NO_x on

$PM_{2.5}$ concentrations. InMAP is a reduced complexity model that can simulate $PM_{2.5}$ concentrations given emissions inputs (*9*) and has been widely used at national scale to identify the levels and disparities in $PM_{2.5}$ (*10*, *11*). More details of the InMAP simulations could be found in SI. Here, we use the InMAP source receptor matrix (ISRM) archived from (*12*). The ISRM consists of matrices of dimensions 52411×52411 (with the US divided into 52411 grid cells) for three heights of emission locations and seven precursor emission species. For a given height and emission species, ISRM calculates the changes in $PM_{2.5}$ for any grid cell in the US due to one unit increase in one of the precursor emissions in any of the 52411 grid cells. We multiply the ISRM of SO_2 and NO_x by the plant-level drought-induced emission changes (emission heights are determined according to the stack heights of the plant) to calculate the changes in drought-induced surface $PM_{2.5}$ for each month.

Projecting future impacts in the *high RE scenario*

Expansions of RE could shift marginal energy sources from fossil energy to non-fossil energy. In our *high RE scenario*, we assume that when non-fossil energy is on the margin, the drought-induced electricity gap will be provided by the non-fossil energy. We assume that if a non-fossil energy source is at the margin for the region where drought occurs, the electricity generation gap will be only provided by the non-fossil energy source from the drought region and therefore the drought region does not need to import electricity from the neighboring region (regardless of the marginal energy source in the neighboring region). Our projection thus assumes that if the non-fossil source is on the margin for a given hour, it will have enough excess generation to cover the electricity gap during drought.

We use the following illustrative example to demonstrate the projections of drought-induced emissions under *high RE* scenario. Our empirical analysis quantifies that an extreme drought in CA (corresponding to the 5th-percentile lowest runoff value from 2001-2021) leads to an increase in electricity generation by 19% from gas-fired plants in CAISO (the CA region), and 11% increase from gas-fired plants in Public Service Company of Colorado (PSCC, part of the NW region). Suppose fossil energy is at the margin in both CAISO and PSCC, we would estimate an 19% increase of generation in CAISO and 11% increase in PSCC due to drought in CA, same as the empirical estimates. If fossil energy is on the margin in CAISO but not in PSCC, we would estimate an 19% increase of gas-fired unit emissions in CAISO, and 0% for PSCC (as the generation gap will be provided by the non-fossil source in PSCC). On the other hand, if fossil energy is on the

margin in PSCC (but not CAISO), then we estimate an 0% emission increase for both regions (as the electricity gap in CA is solely provided by the non-fossil source in the CAISO).

References

1. U.S. Energy Information Administration, *Hourly Electric Grid Monitor*, 2021.

2. D. Tingley, T. Yamamoto, K. Hirose, L. Keele, K. Imai, Mediation: R package for causal mediation analysis. (2014).

3. Y. Wang, Y. Xie, W. Dong, Y. Ming, J. Wang, L. Shen, Adverse effects of increasing drought on air quality via natural processes. *Atmospheric Chemistry and Physics* **17**, 12827–12843 (2017).

4. Y. Xie, M. Lin, B. Decharme, C. Delire, L. W. Horowitz, D. M. Lawrence, F. Li, R. Séférian, Tripling of western US particulate pollution from wildfires in a warming climate. *Proceedings of the National Academy of Sciences* **119**, e2111372119 (2022).

5. M. L. Childs, J. Li, J. Wen, S. Heft-Neal, A. Driscoll, S. Wang, C. F. Gould, M. Qiu, J. Burney, M. Burke, Daily Local-Level Estimates of Ambient Wildfire Smoke PM2. 5 for the Contiguous US. *Environmental Science & Technology* (2022).

6. W. Schroeder, M. Ruminski, I. Csiszar, L. Giglio, E. Prins, C. Schmidt, J. Morisette, Validation analyses of an operational fire monitoring product: The Hazard Mapping System. *International Journal of Remote Sensing* **29**, 6059–6066 (2008).

7. G. D. Rolph, R. R. Draxler, A. F. Stein, A. Taylor, M. G. Ruminski, S. Kondragunta, J. Zeng, H.-C. Huang, G. Manikin, J. T. McQueen, *et al.*, Description and verification of the NOAA smoke forecasting system: the 2007 fire season. *Weather and Forecasting* **24**, 361–378 (2009).

8. M. Ruminski, S. Kondragunta, R. Draxler, J. Zeng, presented at the Proceedings of the 15th International Emission Inventory Conference, vol. 15, p. 18.

9. C. W. Tessum, J. D. Hill, J. D. Marshall, InMAP: A model for air pollution interventions. *PloS one* **12**, e0176131 (2017).

10. C. W. Tessum, J. S. Apte, A. L. Goodkind, N. Z. Muller, K. A. Mullins, D. A. Paolella, S. Polasky, N. P. Springer, S. K. Thakrar, J. D. Marshall, *et al.*, Inequity in consumption of goods and services adds to racial–ethnic disparities in air pollution exposure. *Proceedings of the National Academy of Sciences* **116**, 6001–6006 (2019).

11. C. W. Tessum, D. A. Paolella, S. E. Chambliss, J. S. Apte, J. D. Hill, J. D. Marshall, PM2. 5 polluters disproportionately and systemically affect people of color in the United States. *Science Advances* **7**, eabf4491 (2021).

12. A. L. Goodkind, C. W. Tessum, J. S. Coggins, J. D. Hill, J. D. Marshall, Fine-scale damage estimates of particulate matter air pollution reveal opportunities for location-specific mitigation of emissions. *Proceedings of the National Academy of Sciences* **116**, 8775–8780 (2019).

13. T. Deryugina, G. Heutel, N. H. Miller, D. Molitor, J. Reif, The mortality and medical costs of air pollution: Evidence from changes in wind direction. *American Economic Review* **109**, 4178–4219 (2019).

14. C. Liu, R. Chen, F. Sera, A. M. Vicedo-Cabrera, Y. Guo, S. Tong, M. S. Coelho, P. H. Saldiva, E. Lavigne, P. Matus, *et al.*, Ambient particulate air pollution and daily mortality in 652 cities. *New England Journal of Medicine* **381**, 705–715 (2019).

15. Q. Di, L. Dai, Y. Wang, A. Zanobetti, C. Choirat, J. D. Schwartz, F. Dominici, Association of short-term exposure to air pollution with mortality in older adults. *Jama* **318**, 2446–2456 (2017).

16. P. Orellano, J. Reynoso, N. Quaranta, A. Bardach, A. Ciapponi, Short-term exposure to particulate matter (PM10 and PM2. 5), nitrogen dioxide (NO2), and ozone (O3) and all-cause and cause-specific mortality: Systematic review and meta-analysis. *Environment international* **142**, 105876 (2020).

17. S. L. Decker, Officials identify steam plant accident victim. *The Chronicle* (May 11, 2005).

18. P. Gagnon, W. Frazier, W. Cole, E. Hale, "Cambium Documentation: Version 2021", tech. rep. (National Renewable Energy Lab.(NREL), Golden, CO (United States), 2021).

19. U.S. Environmental Protection Agency, *Emissions and Generation Resource Integrated Database (eGRID) 2019*, 2019.

Supplementary tables

	log (generation)	
	Texas	**Florida**
Runoff	-0.012	-0.008
	(0.012)	(0.021)

Table S1: **Fossil generation in Texas and Florida are not associated with runoff changes in each region.** The table shows the impacts of runoff anomalies on the electricity generation from fossil fuel plants in Texas or Florida. The impacts are estimated using regressions similar to equation [1] in the main text (except for only runoff anomalies from a single region is considered). Standard errors are clustered at the plant level.

Table S2: **Climate models used in this study for future projections.** The spatial resolution of each model is shown in latitude × longitude (unit: degree). Resolutions are approximated for models with varying latitudes. Data is downloaded in October, 2022.

Model	**Ensemble variant**	**Resolution**
ACCESS-CM2	r1i1p1f1	1.25 x 1.88
ACCESS-ESM1-5	r1i1p1f1	1.25 x 1.88
BCC-CSM2-MR	r1i1p1f1	1.12 x 1.12
CanESM5	r1i1p1f1	2.79 x 2.81
CAS-ESM2-0	r1i1p1f1	1.42 x 1.41
CESM2-WACCM	r1i1p1f1	0.94 x 1.25
CMCC-CM2-SR5	r1i1p1f1	0.94 x 1.25
CMCC-ESM2	r1i1p1f1	0.94 x 1.25
CNRM-CM6-1	r1i1p1f2	1.4 x 1.41
CNRM-CM6-1-HR	r1i1p1f2	0.5 x 0.5
CNRM-ESM2-1	r1i1p1f2	1.4 x 1.41
EC-Earth3	r1i1p1f1	0.7 x 0.7
EC-Earth3-Veg	r1i1p1f1	0.7 x 0.7
EC-Earth3-Veg-LR	r1i1p1f1	1.12 x 1.12
FGOALS-f3-L	r1i1p1f1	0.94 x 1.25
FGOALS-g3	r1i1p1f1	2.03 x 2
GFDL-ESM4	r1i1p1f1	1 x 1.25
GISS-E2-1-G	r1i1p1f2	2 x 2.5
GISS-E2-1-H	r1i1p1f2	2 x 2.5
INM-CM4-8	r1i1p1f1	1.5 x 2
INM-CM5-0	r1i1p1f1	1.5 x 2
IPSL-CM6A-LR	r1i1p1f1	1.27 x 2.5
KACE-1-0-G	r1i1p1f1	1.25 x 1.88
MCM-UA-1-0	r1i1p1f2	2.24 x 3.75
MIROC-ES2L	r1i1p1f2	2.79 x 2.81
MIROC6	r1i1p1f1	1.4 x 1.41
MPI-ESM1-2-HR	r1i1p1f1	0.94 x 0.94
MPI-ESM1-2-LR	r1i1p1f1	1.87 x 1.88
MRI-ESM2-0	r1i1p1f1	1.12 x 1.12
NorESM2-LM	r1i1p1f1	1.89 x 2.5
NorESM2-MM	r1i1p1f1	0.94 x 1.25
TaiESM1	r1i1p1f1	0.94 x 1.25
UKESM1-0-LL	r1i1p1f2	1.25 x 1.88

Supplementary figures

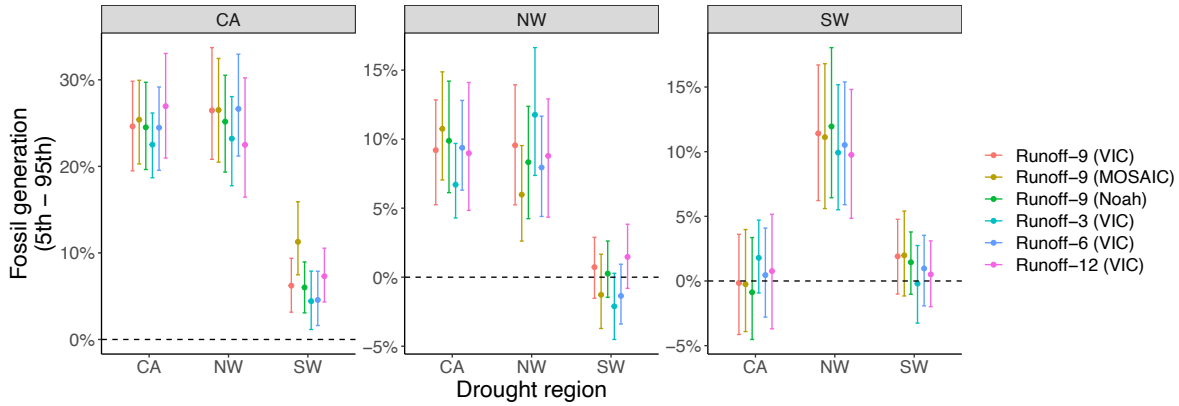

Figure S1: **Estimation results using runoff anomalies calculated using alternative methods.** Figure shows the estimated changes in fossil generation in one electricity region (corresponding to each panel) due to the 5th to 95th percentile change of runoff in each of the three regions (x-axis of each panel). The error bars show the 95% confidence intervals of the estimated generation changes. Standard errors are clustered at the plant level. Estimation results using runoff anomalies calculated with different methods are shown in different colors. Runoff anomalies are calculated using different averaging windows (3, 6, 9, 12 months) and derived from three different models of NLDAS-2 (VIC, MOSAIC, Noah). Our main analysis uses 9-month runoff anomalies from the VIC model (Red color, *Runoff-9 (VIC)*).

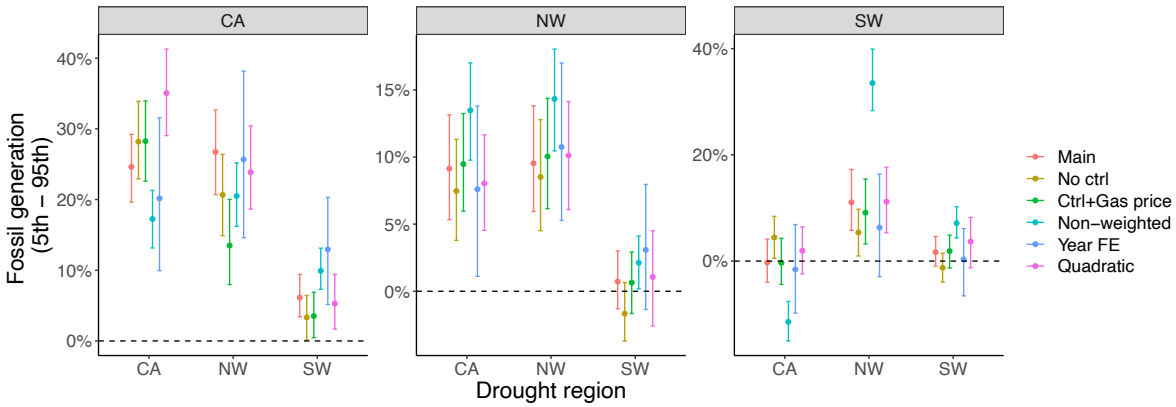

Figure S2: **Estimation results using alternative specifications of the regression model.** Figure shows the estimated changes in fossil generation in one electricity region (corresponding to each panel) due to the 5th to 95th percentile change of runoff in each of the three regions (x-axis of each panel). The error bars show the 95% confidence intervals of the estimated generation changes. Standard errors are clustered at the plant level. Estimation results using alternative specifications of the regression model are shown in different colors. Descriptions of the alternative specifications are discussed in SI.

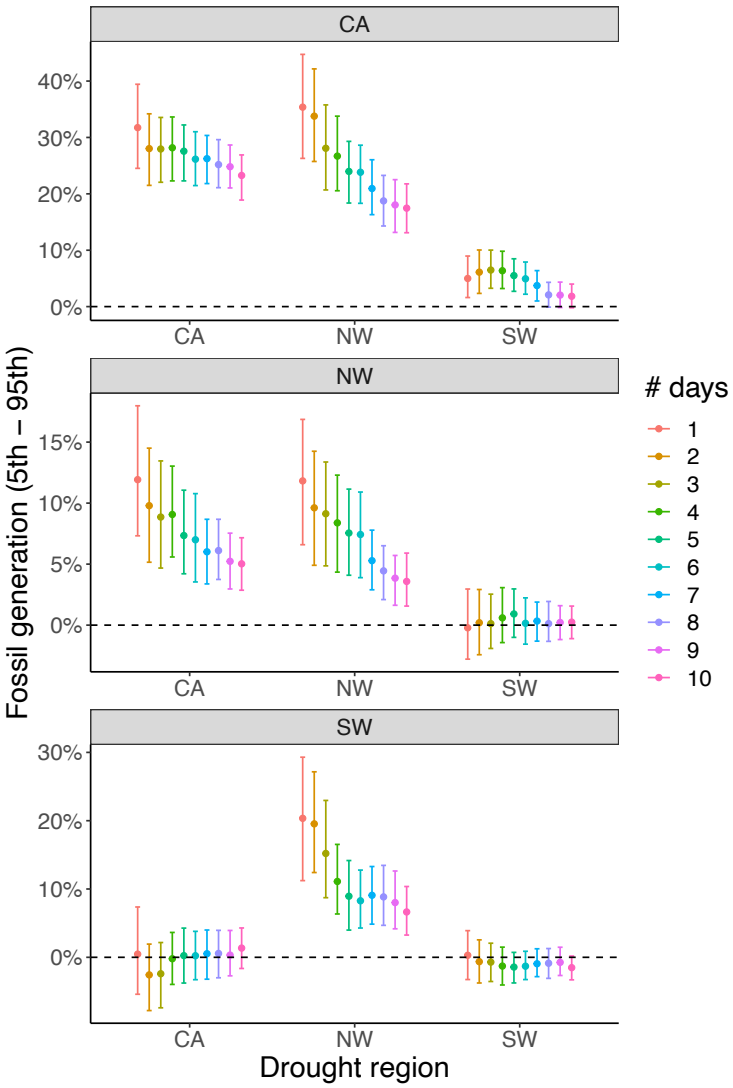

Figure S3: **Estimation results across different sample restrictions.** Figure shows the estimated changes in fossil generation in one electricity region (corresponding to each panel) due to the 5th to 95th percentile change of runoff in each of the three regions (x-axis of each panel). The error bars show the 95% confidence intervals of the estimated generation changes. Standard errors are clustered at the plant level. Estimation results using different criterion for sample restrictions are shown in different colors. Figure shows the estimation results across different sample restrictions. For each estimation, the estimation is performed on the sample that includes an observation only if the unit has operated or reported for at least X days during the month (X=1,..,10). Our main analysis only includes an observation if the unit has operated or reported for at least four days during the month (i.e. X=4).

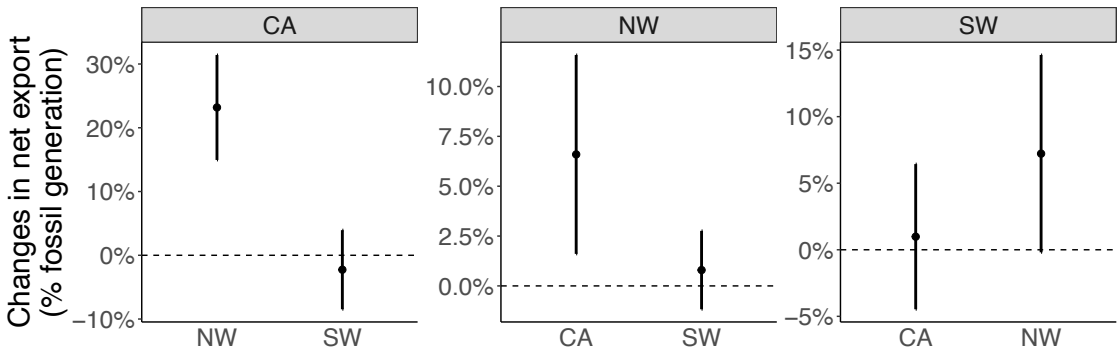

Figure S4: **Drought increases the net export of electricity from the neighboring regions to the drought region.** Figure shows the estimated changes in the net export of electricity from one electricity region (the source region, corresponding to each panel) to another electricity region (the drought region, x-axis of each panel) due to the 5th to 95th percentile change of runoff in the drought region. We use the hourly electricity import and export data from EIA (2016 to 2021) to estimate how drought influences the interregional electricity exchange (*1*).

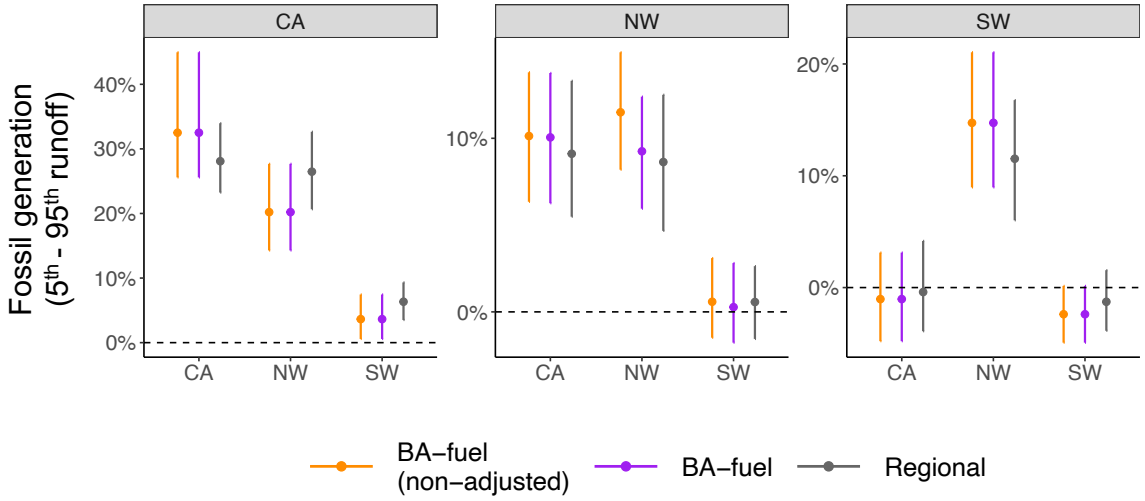

Figure S5: **Estimated impacts on fossil fuel generation are consistent across the estimations at the regional level and BA-fuel level.** Changes in electricity generation estimated using the coefficients derived from regressions at the BA-fuel level are shown in orange. Changes in electricity generation estimated with adjusted coefficients (for 11 out of 681 units, we use the pooled regression coefficients at the regional level instead of the highly uncertain coefficients estimated at the BA-fuel level) are shown in purple. Changes in electricity generation estimated using the coefficients derived from the pooled regressions are shown in grey.

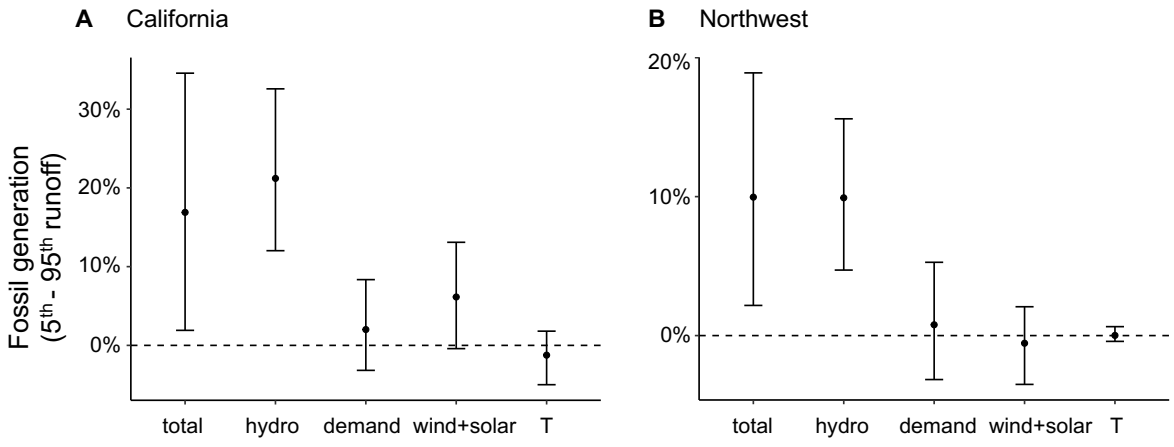

Figure S6: **The need to substitute for changes in hydro power is the leading mechanism that explains the runoff – fossil generation relationship.** Figure shows the changes in fossil fuel generation associated with changes due to the 5th to 95th percentile change of runoff anomalies, through different mechanisms. We only focus on the drought impacts on fossil fuel plants in the same electricity region (i.e. the local effect), and only focus on California and Northwest where the estimated local effects are substantial. Figure shows the effects through all possible mechanisms ('total'), effects through changes in hydropower ('hydro'), effects through changes in electricity demand ('demand'), effects through changes in wind and solar generation ('wind+solar'), and effects through changes in the local temperature at the plant locations ('T', possibly by influencing the cooling efficiency).

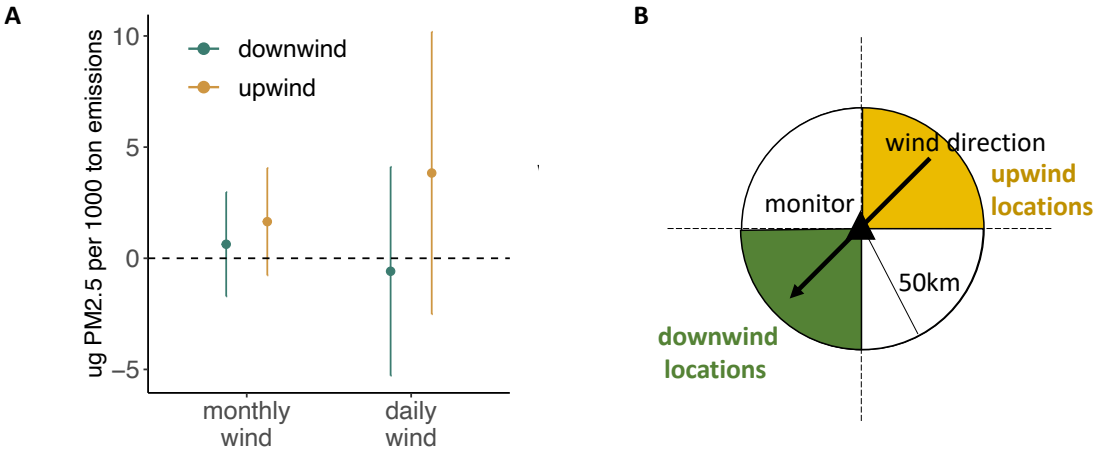

Figure S7: **Increases in surface $PM_{2.5}$ are more likely to be associated with drought-induced emission emitted from upwind plants.** Panel A shows the $PM_{2.5}$ impacts of drought-induced emissions from fossil fuel plant within 50km radius of the monitor at upwind or downwind locations of the monitor. As shown in panel B, a plant is determined to be at the upwind location, if the plant is located in the "upwind quadrant" which is a 90 degree cone centering around the wind direction. The wind direction is calculated using the zonal and meridional wind components within 50km of the monitor (wind direction derived from the ERA5 land reanalysis data). Panel A shows the results estimated using monthly-average wind direction, as well as daily wind direction (paired with drought-induced emissions calculated at the daily level).

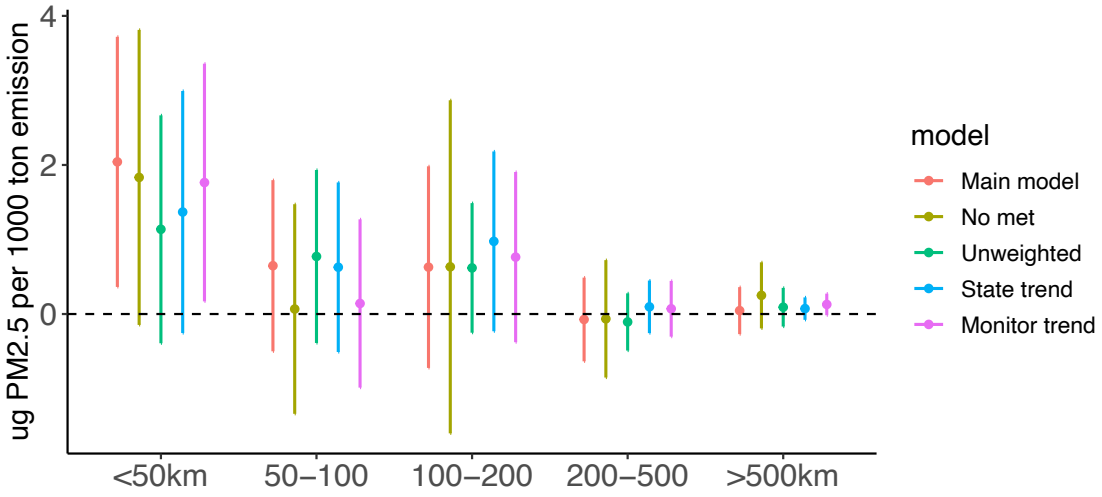

Figure S8: **Estimated impacts of drought-induced emission on surface $PM_{2.5}$ are largely consistent across alternative model specifications.** In our main specification, we include the splines of surface temperature, precipitation, dewpoint temperature, boundary layer height, air pressure, 10m wind direction (U and V components) and wind speed for meteorological controls, year and month-of-year fixed effects. The figure shows coefficients estimated with no meteorology controls ('No met'), coefficient estimated using ordinary least square ('Unweighted'), and coefficient estimated using state-level year trend ('State trend') or monitor-level year trend ('Monitor trend') instead of the year fixed effects.

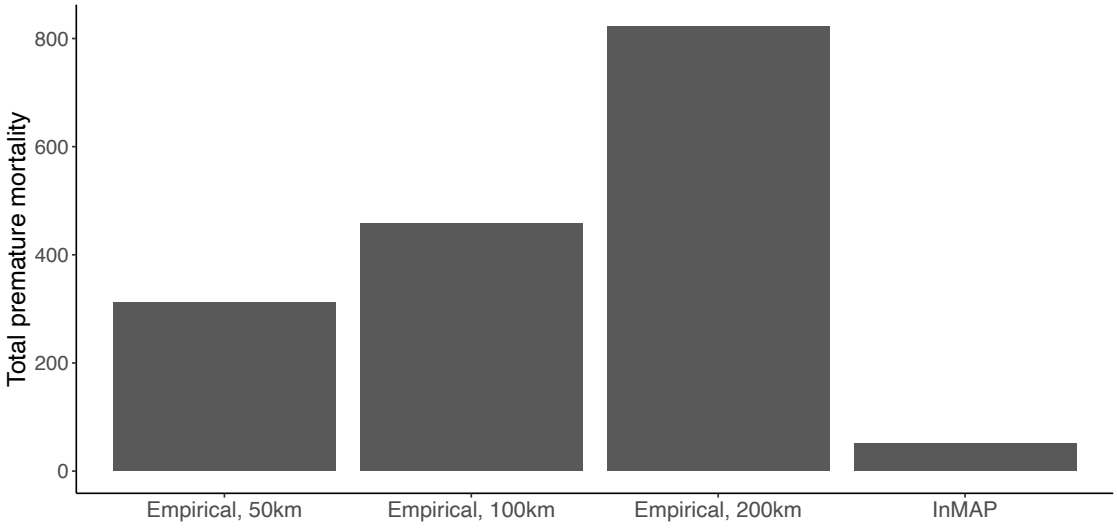

Figure S9: **Total premature mortalities due to drought-induced fossil generation during 2001 to 2021, calculated using different methods to estimate drought-induced $PM_{2.5}$.** The figure shows three empirical estimates and one estimate based on InMAP simulations of the drought-induced $PM_{2.5}$ mortalities. Mortalities are estimated using the same CRF function from Deryugina et al. For the empirical estimates of drought-induced $PM_{2.5}$, we consider impacts of drought-induced emissions within the radius of 50km, 100km, or 200km, and use the corresponding regression coefficients. Our main analysis calculates the drought-induced $PM_{2.5}$ using the empirical estimates of the 100km radius.

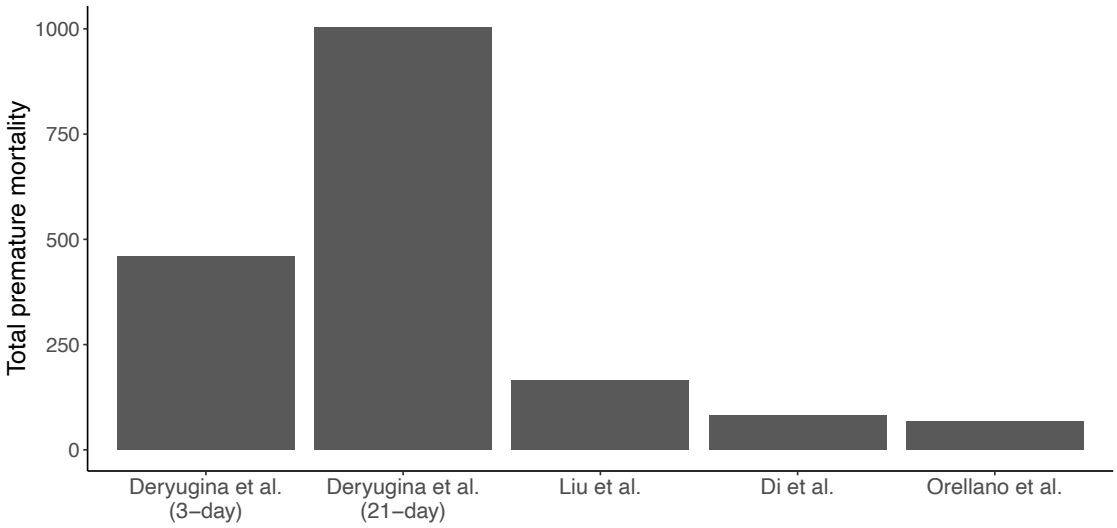

Figure S10: **Total premature mortalities due to drought-induced fossil generation during 2001 to 2021, estimated using different CRFs (*13*–*16*).** *Deryugina et al., (3-day)* uses the main estimate from Deryugina et al. which calculates the total cumulative mortalities in the 3-day window following a day of exposure. *Deryugina et al., (21-day)* uses the alternative estimate reported in Deryugina et al. which calculates the total cumulative mortalities in the 21-day window following a day of exposure. Mortalities are calculated using the estimated drought-induced $PM_{2.5}$ from the empirical approach that accounts for drought-induced emissions within a 100km radius.

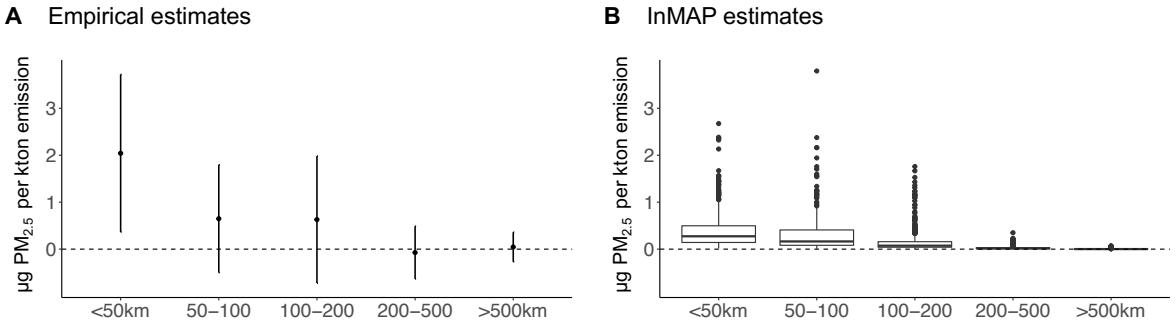

Figure S11: **Empirical and InMAP estimates of $PM_{2.5}$ impacts associated with drought-induced emissions.** Panel A shows the empirical estimates of drought-induced emissions of different distance bins on surface $PM_{2.5}$ (same as figure 3C in the main text). Panel B shows the InMAP estimates of drought-induced emissions on surface $PM_{2.5}$. To derive the InMAP estimates, we first use InMAP to simulate the $PM_{2.5}$ changes in the Western US associated with one ton of SO_2 and NO_x emissions emitted from all power plants in our sample. Then for each air quality monitor, we calculate the ratio between the simulated $PM_{2.5}$ and the emissions from plants of a certain distance bin. The box plot in Panel B shows the range of the $PM_{2.5}$ – emissions sensitivities across different monitor locations.

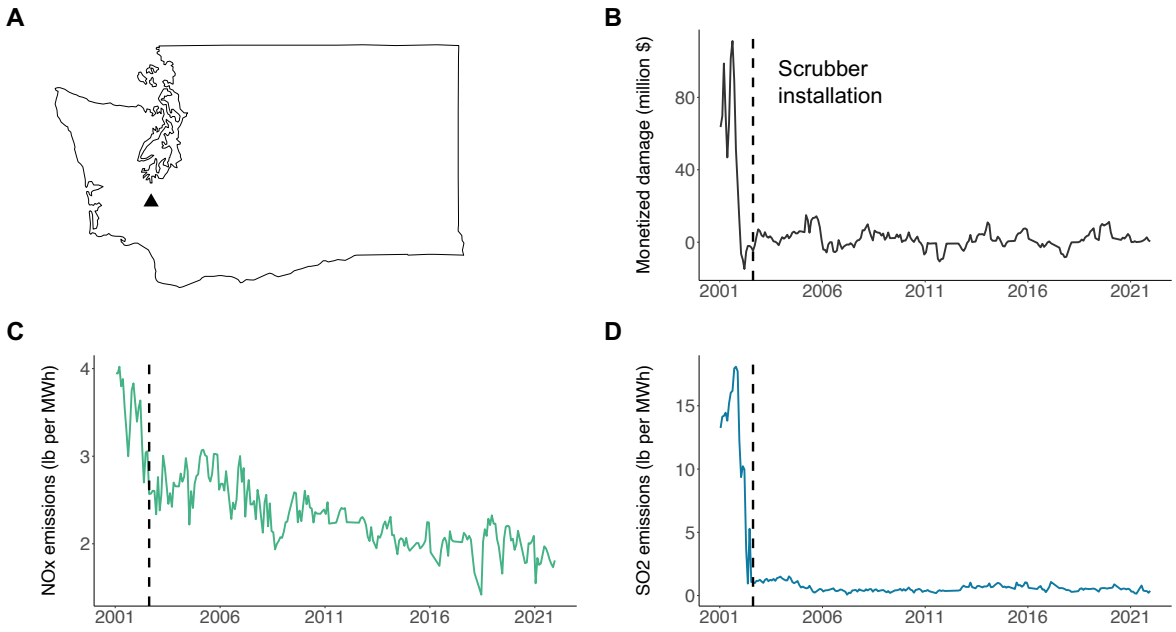

Figure S12: **Dramatic declines in the drought-induced $PM_{2.5}$ damage are driven by decline in emissions factors after scrubber installations.** Results are shown for a power plant in the Washington State (panel A), which includes two units using coal as their main fuel type. Panel B shows the $PM_{2.5}$ damage due to the drought-induced emission changes from this plant, driven by dramatic declines in NO_x and SO_2 emission factors (panel C and D) after the installation of scrubbers on August, 2002 (*17*).

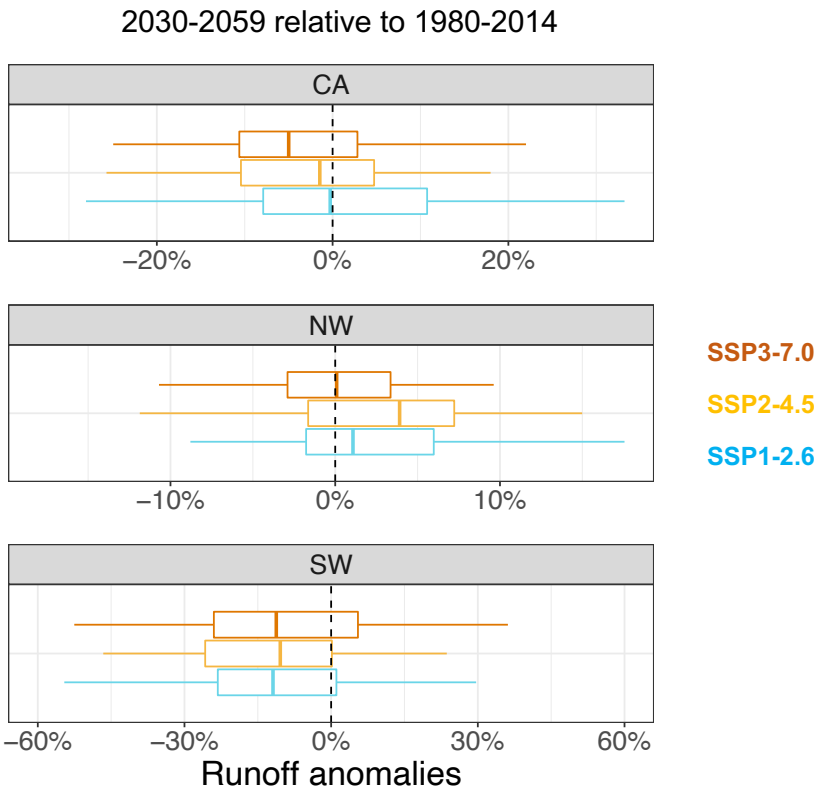

Figure S13: **Projected runoff anomalies under future climate.** The box plots show the range of projected runoff anomalies from 33 global climate models in CMIP6, under SSP1-2.6, SSP2-4.5, and SSP3-7.0 scenarios. Runoff anomalies are calculated relative to the 1980-2014 values from the historical simulations and then averaged over 2030-2059.

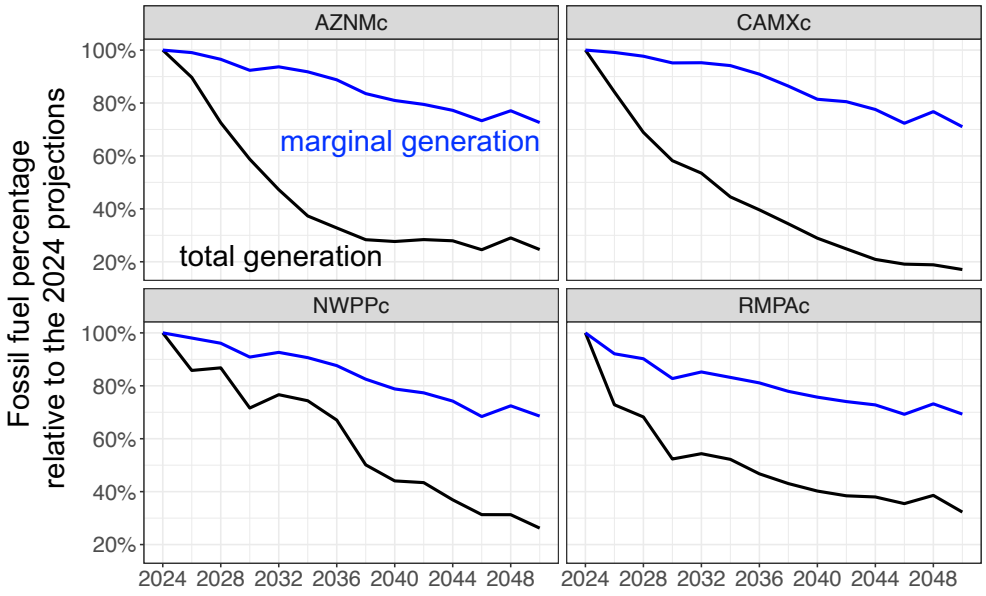

Figure S14: **Projected percentages of fossil fuel generation in the electricity grid of western US.** We calculate the ratio of fossil fuel generation relative to the total electricity generation (black), and the percentage of time that fossil fuel generators being the marginal generators of the electric grid (blue). Results are derived from the hourly simulation under the "Low RE cost scenarios" of the Cambium data sets from 2024 to 2050 (*18*). Figures show the changes in fossil fuel generation percentage relative to the 2024 projections (2024 results normalized to 1), for the four egrid subregions of western US (*19*).

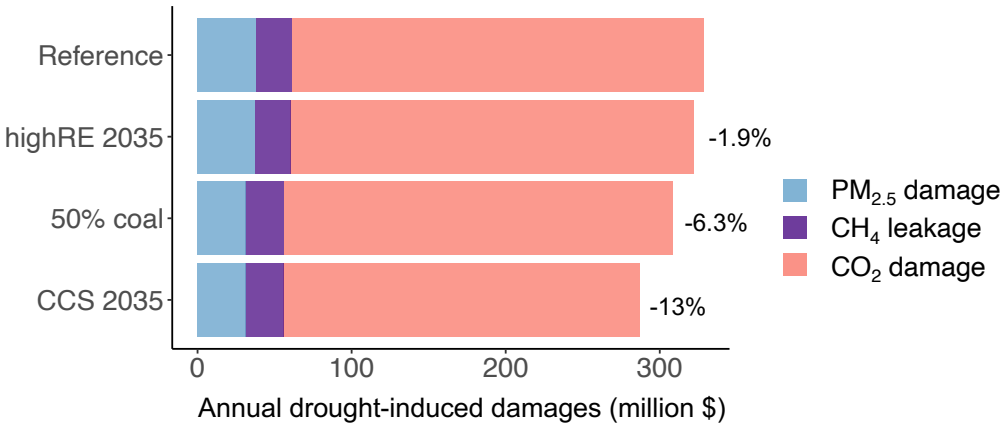

Figure S15: **Modest reductions in drought-induced damages under projected electricity sector scenarios (projection year 2035).** Figure shows the mean values of drought-induced damages projected by the 33 models under SSP3-7.0. The relative difference of damages under the three electricity sector scenarios (compared to the reference scenario) is shown in the figure.

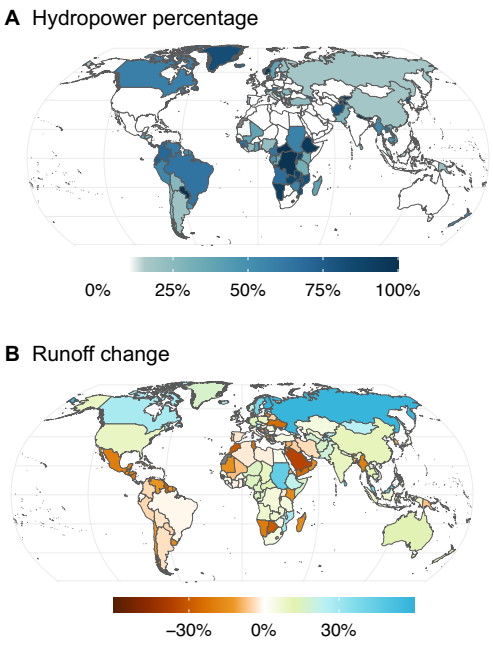

C

Country	Hydropower percentage	Runoff change
Namibia	93%	-21%
Bhutan	100%	-20%
Honduras	30%	-20%
Burma	53%	-19%
Guatemala	38%	-17%
Uruguay	47%	-17%
Kenya	33%	-16%
Madagascar	40%	-16%
French Guiana	48%	-16%
Venezuela	62%	-13%
Suriname	52%	-13%
Chile	25%	-12%
El Salvador	27%	-8%
Bosnia and Herzegovina	31%	-8%
Mali	39%	-7%
Papua New Guinea	21%	-7%
Portugal	20%	-7%
Fiji	50%	-7%
The former Yugoslav Republic of Macedonia	26%	-5%

Figure S16: **Many hydro-dependent countries face increased drought risks due to climate change.** Panel A shows the percentage of electricity provided by hydropower of each country (averaged over 2015-2021). Panel B shows the projected changes (median changes across 33 models) in runoff of each country under SSP3-7.0 between 2030 to 2059 (relative to 1980 to 2014). We identify 19 countries (table C) that could be vulnerable to drought-induced shocks to the electricity system (with >5% decline in runoff and >20% generation coming from hydropower).